

Role of Activating Transcription Factor 3 on TAp73 Stability and Apoptosis in Paclitaxel-Treated Cervical Cancer Cells

Yeo Kyoung Oh,¹ Hyun Jung Lee,¹ Mi-Hee Jeong,² Marie Rhee,¹ Ji-Won Mo,¹ Eun Hyeon Song,¹ Joong-Yeon Lim,¹ Kyung-Hee Choi,² Inho Jo,³ Sang Ick Park,¹ Bin Gao,⁴ Yongil Kwon,⁵ and Won-Ho Kim¹

¹Division of Intractable Diseases, Center for Biomedical Sciences, NIH, ²Laboratory of Molecular Biology, Department of Biology, College of Natural Science, Chung-Ang University, ³Department of Molecular Medicine, School of Medicine, Ewha Womans University, Seoul, Korea; ⁴Section on Liver Biology, Laboratory of Physiologic Studies, National Institute on Alcohol Abuse and Alcoholism, NIH, Bethesda, Maryland; and ⁵Gynecologic Oncology, Kangdong Sacred Heart Hospital, Hallym University, Seoul, Korea

Abstract

Taxol (paclitaxel) is a potent anticancer drug that has been found to be effective against several tumor types, including cervical cancer. However, the exact mechanism underlying the antitumor effects of paclitaxel is poorly understood. Here, paclitaxel induced the apoptosis of cervical cancer HeLa cells and correlated with the enhanced activation of caspase-3 and TAp73, which was strongly inhibited by TAp73 β small interfering RNA (siRNA). In wild-type activating transcription factor 3 (ATF3)-overexpressed cells, paclitaxel enhanced apoptosis through increased α and β isoform expression of TAp73; however, these events were attenuated in cells containing inactive COOH-terminal-deleted ATF3 [ATF3(Δ C)] or ATF3 siRNA. In contrast, paclitaxel-induced ATF3 expression did not change in TAp73 β -overexpressed or TAp73 β siRNA-cotransfected cells. Furthermore, paclitaxel-induced ATF3 translocated into the nucleus where TAp73 β is expressed, but not in ATF3(Δ C) or TAp73 β siRNA-transfected cells. As confirmed by the GST pull-down assay, ATF3 bound to the DNA-binding domain of p73, resulting in the activation of p21 or Bax transcription, a downstream target of p73. Overexpression of ATF3 prolonged the half-life of TAp73 β by inhibiting its ubiquitination and thereby enhancing its transactivation and proapoptotic activities. Additionally, ATF3 induced by paclitaxel potentiated the stability of TAp73 β , not its

transcriptional level. Chromatin immunoprecipitation analyses show that TAp73 β and ATF3 are recruited directly to the p21 and Bax promoter. Collectively, these results reveal that overexpression of ATF3 potentiates paclitaxel-induced apoptosis of HeLa cells, at least in part, by enhancing TAp73 β 's stability and its transcriptional activity. The investigation shows that ATF3 may function as a tumor-inhibiting factor through direct regulatory effects on TAp73 β , suggesting a functional link between ATF3 and TAp73 β . (Mol Cancer Res 2008;6(7):1232-49)

Introduction

Paclitaxel is derived from the needles and bark of the Western yew tree (1, 2). It is widely used to treat a variety of solid tumors including ovarian, breast, non-small cell lung carcinomas, and Kaposi's sarcoma (3). The antitumor effects of paclitaxel are mediated by binding to and stabilizing microtubules, thereby enhancing microtubule polymerization leading to G₂-M cell cycle arrest and ultimately to apoptotic cell death (4). Apoptotic tumor cell death is commonly observed in paclitaxel therapy (5); however, the exact mechanisms by which paclitaxel triggers p53-independent apoptosis are not clearly elucidated. Although treatment with paclitaxel can improve survival and quality of life for patients with cancer (6, 7), the majority of patients will eventually experience disease progression even after initially responding to paclitaxel (8).

Unlike p53, the p73 gene is able to encode transcriptionally active TAp73, as well as an NH₂-terminally truncated form, Δ Np73 (DNp73), lacking the transactivation domain (9). TAp73 is expressed as several isoforms, designated as p73 α , p73 β , p73 γ , and p73 δ , due to extensive splicing at the carboxy terminal domain (10). Moreover, not all of the same signals that activate p53 can induce p73 overexpression. Only a subset of DNA-damaging signals that increase p53 expression, such as irradiation or anticancer drugs including cisplatin, camptothecin, paclitaxel, and doxorubicin have been shown to induce TAp73 protein expression (11, 12). In addition, steady-state levels of TAp73 are not reduced by complex formation with Mdm2 (13), which targets p53 for ubiquitin-mediated proteolysis (14).

Received 6/27/07; revised 3/5/08; accepted 4/10/08.

Grant support: Korean NIH (4845-300-210-13).

The costs of publication of this article were defrayed in part by the payment of page charges. This article must therefore be hereby marked *advertisement* in accordance with 18 U.S.C. Section 1734 solely to indicate this fact.

Note: Supplementary data for this article are available at Molecular Cancer Research Online (<http://mcr.aacrjournals.org/>).

Y.K. Oh and H.J. Lee contributed equally to this work.

Requests for reprints: Won Ho Kim, Division of Intractable Diseases, Center for Biomedical Sciences, NIH, no. 194 Tongillo, Eunpyeong-gu, Seoul 122-701, Korea. Phone: 82-2380-1528; Fax: 82-2388-0924. E-mail: jhkwh@nih.go.kr or Yongil Kwon, Gynecologic Oncology, Kangdong Sacred Heart Hospital, Hallym University, Seoul 134-701, Korea. E-mail: kbg@hallym.or.kr

Copyright © 2008 American Association for Cancer Research.
doi:10.1158/1541-7786.MCR-07-0297

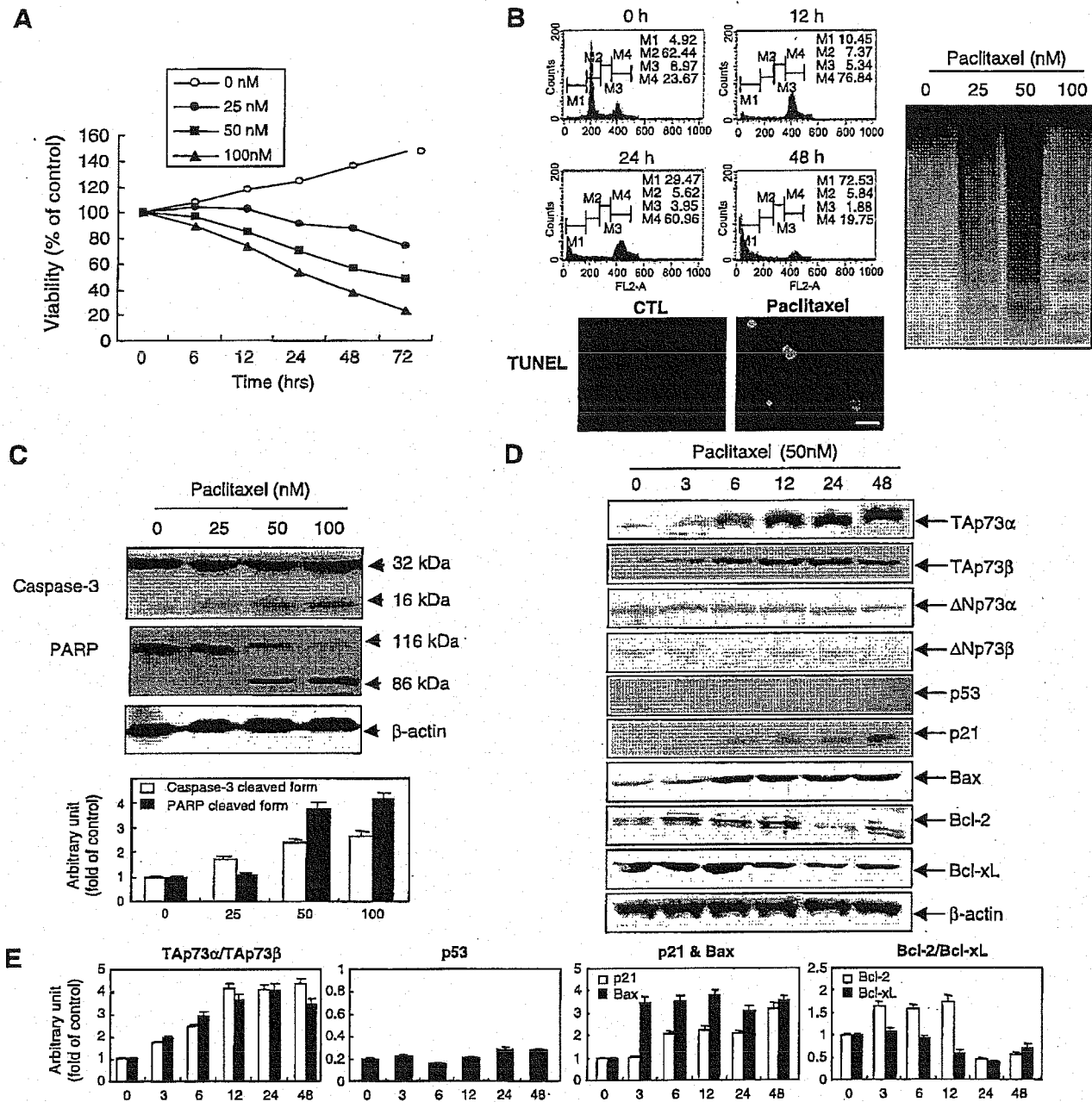


FIGURE 1. The effects of paclitaxel on apoptosis in cervical cancer cells. HeLa cells were treated with different paclitaxel concentrations for the indicated times. **A.** MTT assay. **B.** Apoptosis ($M1$, sub-G1 peak) was measured by propidium iodide staining (top), TUNEL assay (bottom; bar, 10 μ m), DNA fragmentation (right). **C.** The cleavage of caspase-3 and poly(ADP-ribose) polymerase was analyzed. Expression (**D**) and quantification (**E**) of apoptosis-related proteins in HeLa cells. Whole-cell lysates were separated on SDS-PAGE, followed by Western blotting using the specific antibodies. Similar results were obtained for each of the three experiments.

Recent studies have shown that despite disruption in p53 and pRB functioning by E6 and E7 oncoproteins associated with cervical cancer caused by the human papillomavirus (HPV), the TAp73 gene was overexpressed in both radiosensitive and radioresistant cervical cancers (15, 16). Moreover, activated p73 in the absence of functional p53 activates the transcription of p53 target genes such as p21 or Bax, and induces apoptosis in p53-null SAOS2 cells (17). In

cervical cancers in which p53 is impaired, it is therefore reasonable to postulate that in response to paclitaxel, TAp73 overexpression is a compensatory mechanism necessary to trigger p53-independent apoptosis. Thus, if TAp73 is functionally active in paclitaxel-treated cervical cancer cells, it may be important to understand the molecular mechanisms involved in the regulation of the TAp73 gene and its downstream effects.

Transcription factors play key roles in controlling cell proliferation, cell cycle progression, and apoptosis (18, 19), and are therefore subject to targeting by therapeutic drugs. In particular, activating transcription factor 3 (ATF3), which is a member of the ATF/cyclic AMP-responsive element binding protein subfamily, is a stress-inducible transcriptional repressor (20) as well as a basic region-leucine zipper transcription factor. It is induced in cells exposed to a variety of stressful stimuli (e.g., toxic chemicals, anticancer drugs, proteasome inhibitors, genotoxic agents, homocysteine, and ischemia reperfusion) and causes cell cycle arrest and apoptotic cell death (21, 22). It was recently reported that ATF3 transcription is regulated by a variety of signaling pathways and transcription factors, including nuclear factor κ B, EGR-1, and *c-Jun*-NH₂-kinase (23). Moreover, topoisomerase inhibitor, etoposide, as well as camptothecin-induced apoptosis and caspase activity are both potentiated by ATF3 overexpression in human epitheloid carcinoma HeLa-S3 cells (24). Recently, ATF3 has been found to interact with p53 proteins stimulated by genotoxic stress and prevent p53 ubiquitination and degradation, which consequently augments p53 function and results in enhanced apoptosis (25). In contrast, there is some evidence showing that ATF3

inhibits doxorubicin-induced apoptosis through down-regulation of p53 in cardiac myocytes (26). Although the induction of ATF3 by stress signals is neither tissue-specific nor stimulus-specific, they all induce cellular damage (27). Therefore, we hypothesize that TAp73 contributes to apoptosis induced by paclitaxel in cervical cancer cells and that ATF3 may potentially be a major regulator of p73 expression.

In this investigation, we showed that ATF3 overexpression potentiates paclitaxel-induced apoptosis of cervical cancer HeLa cells, at least in part, through stimulating TAp73 expression and transcriptional activity. Furthermore, ATF3 interacted directly with TAp73 and enhanced the stability of the latter, and therefore, it may serve as a tumor-inhibiting factor via stimulation of the apoptotic functions of TAp73. Here, we show for the first time that TAp73 is physically, as well as functionally, associated with the novel stress-inducible transcription factor ATF3.

Results

Paclitaxel Induces Apoptosis in HeLa Cells

To examine the molecular mechanisms involved in the cytotoxic effects of paclitaxel on a human cervical cancer cell

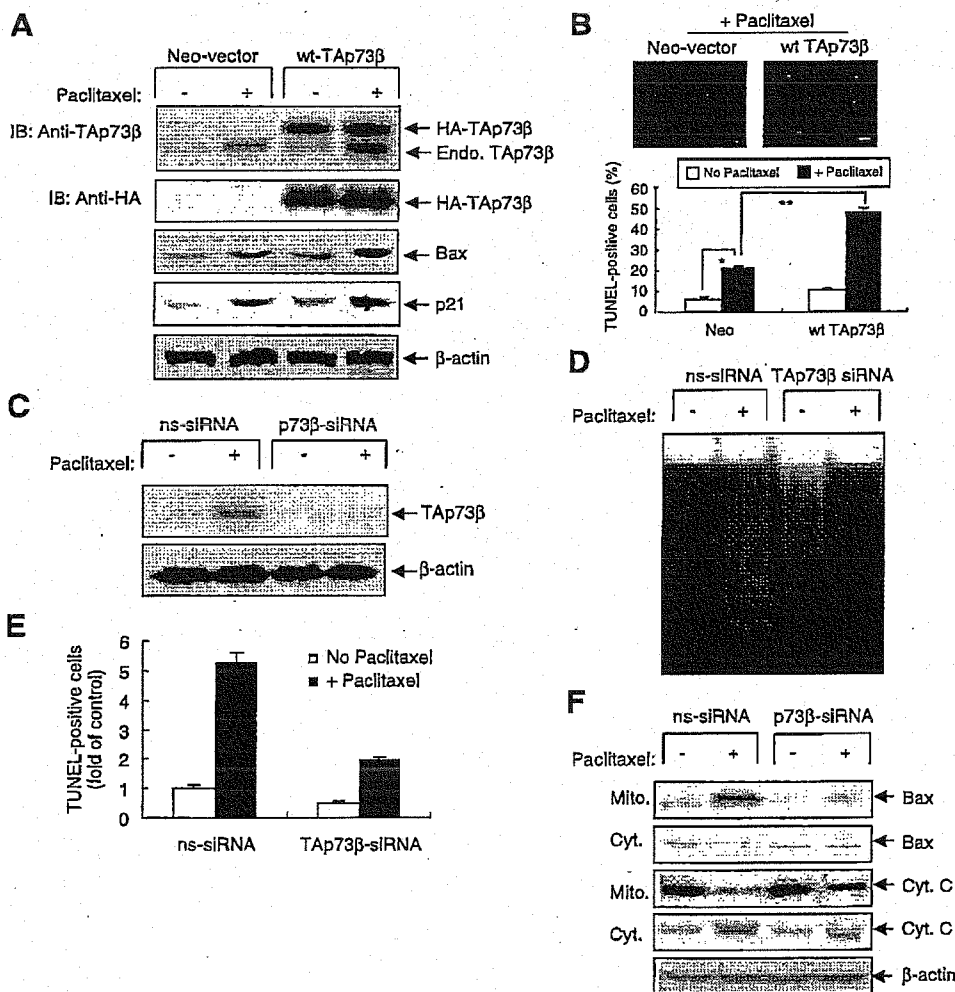
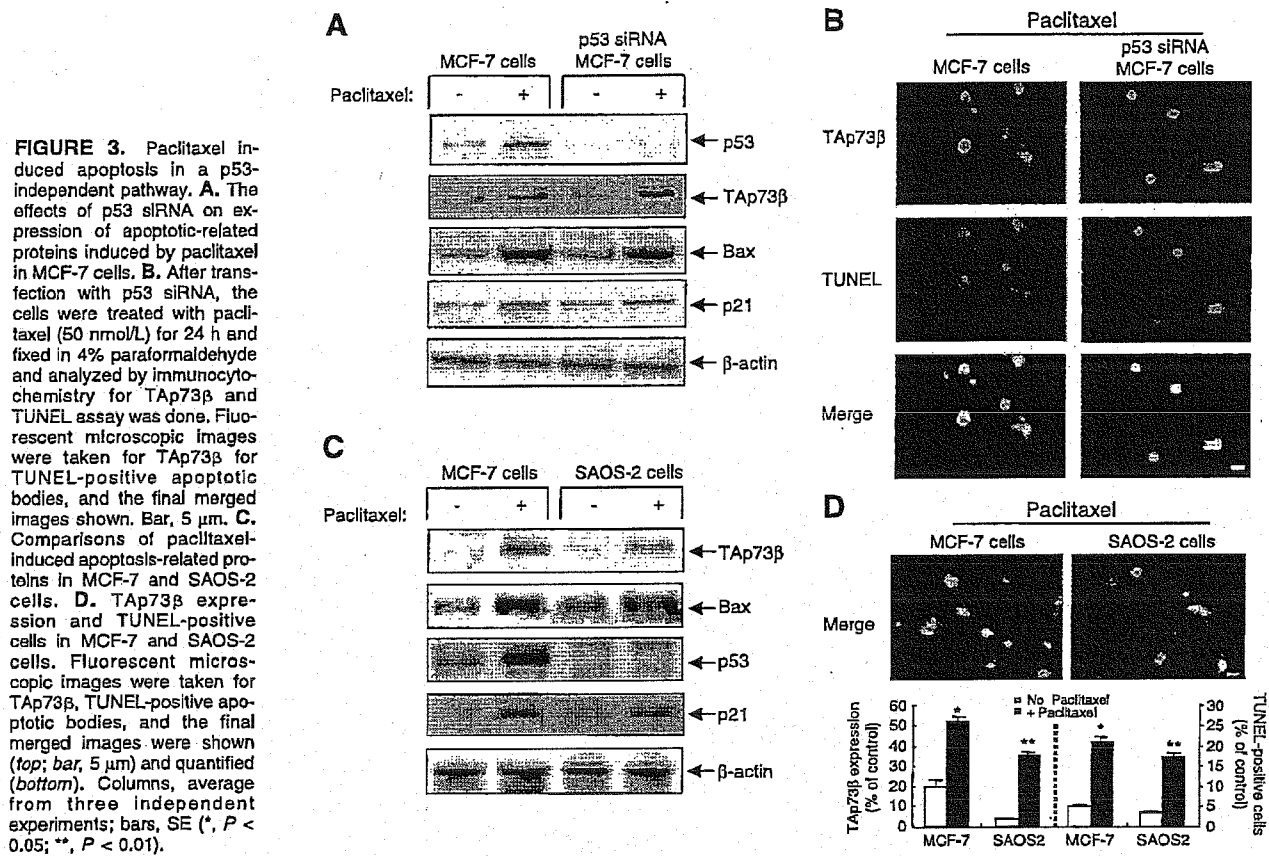


FIGURE 2. The effects of wild-type TAp73 β or TAp73 β siRNA transfection on paclitaxel-induced apoptosis in HeLa cells. **A.** After transfection with either an empty Neo- or wild-type TAp73 β expression vector, the cells were treated with paclitaxel (50 nM) for 24 h. Whole-cell lysates were separated on SDS-PAGE, followed by immunoblotting using specific antibodies. **B.** Apoptotic cells induced by paclitaxel in Neo- or wild-type TAp73 β -transfected cells were analyzed by the TUNEL assay (top; bar, 10 μ m) and quantified (bottom). Columns, average from three independent experiments; bars, SE (*, $P < 0.05$; **, $P < 0.01$). **C** and **D.** The effects of TAp73 β siRNA on TAp73 β expression and DNA fragmentation induced by paclitaxel. **E.** TAp73 β siRNA prevented paclitaxel-induced TUNEL-positive apoptotic cells. Columns, average from three independent experiments; bars, SE (*, $P < 0.05$; **, $P < 0.01$). **F.** The effect of TAp73 β siRNA on expression of apoptosis-related proteins in HeLa cells. After incubation with paclitaxel in the absence or presence of TAp73 β siRNA, mitochondrial and cytosolic fractions were separated and Bax and cytochrome *c* contents were analyzed by Western blotting. Similar results were obtained for each of the three experiments.



line, we first screened three different human-derived cervical cancer cell lines, HeLa, SiHa, and Caski, following treatment with paclitaxel at different concentrations for varying time periods. All of the screened cell types revealed high cytotoxicity to paclitaxel in a time-dependent and dose-dependent manner (data not shown). In particular, HeLa cells seemed to be the most sensitive among the panel of cell lines evaluated and was therefore chosen for our experiments. Cell viability measured by the 3-(4,5-dimethylthiazol-2-yl)-2,5-diphenyltetrazolium bromide assay revealed that paclitaxel (25 and 50 nmol/L) induced 9% and 24.6% cytotoxicity, respectively, after 24 hours (Fig. 1A). The majority of the cells were arrested in the G₂-M phase (M4, G₂-M phase; 76.84 \pm 0.05%) 12 h after treatment with paclitaxel. Treatment with 50 nmol/L paclitaxel for 24 hours caused marked apoptosis based on DNA content as measured by fluorescence-activated cell sorting analysis (M1, sub-G₁ phase, 29.47 \pm 0.05% in paclitaxel-treated cells versus 4.92 \pm 0.05% in control cells), whereas most of cells died after 48 hours (M1, 72.53 \pm 0.05%). Similarly, paclitaxel significantly increased terminal nucleotidyl transferase-mediated nick end labeling (TUNEL)-positive apoptotic cells and genomic DNA fragmentation dose-dependently (Fig. 1B). The activity of caspase-3-like proteases was significantly increased in a dose-dependent manner, correlating with cleavage of poly(ADP-ribose) polymerase (Fig. 1C) and consequently led to the release of cytochrome *c* from the mitochondria (data not shown).

Next, we examined the effects of paclitaxel on the expression profile of apoptosis-related proteins in HeLa cells. As shown in Fig. 1D and E, TAp73 α and TAp73 β were strongly induced by paclitaxel, whereas p53 was weakly induced, consistent with previous reports showing that p53 bound to viral proteins such as HPV E6 oncogene are inactivated in HeLa cells (20). Despite minimal p53 expression, p21, a downstream target gene of p53 and p73 (21, 28), was also induced by paclitaxel, suggesting that TAp73 α and TAp73 β might be principally responsible for the induction of p21 in the absence of p53. On the other hand, our data show that these inductions of TAp73 α and TAp73 β are specific because the expressions of dominant negative Δ Np73 α and Δ Np73 β , which were revealed in a variety of tumors (9, 10), were not changed by paclitaxel. Unexpectedly, paclitaxel also increased the antiapoptotic Bcl-2 protein, which was down-regulated after 24 hours, along with the proapoptotic Bax protein; however, another antiapoptotic protein, Bcl-xL, was down-regulated by paclitaxel in a time-dependent manner.

p73 Plays an Important Role in Paclitaxel-Induced Apoptosis

To determine the roles of TAp73 on paclitaxel-induced apoptosis, HeLa cells were transfected with wild-type TAp73 β expression vectors and subsequently treated with paclitaxel. As shown in Fig. 2A, after 24 hours, endogenous TAp73 β

expression increased in Neo vector-transfected cells, but was synergistically potentiated in wild-type TAp73 β -transfected HeLa cells. Additionally, the expression of Bax and p21 increased in wild-type TAp73 β -transfected cells compared with Neo vector-transfected cells. Similarly, TUNEL-positive apoptotic cells induced by paclitaxel increased significantly in wild-type TAp73 β -transfected cells, whereas fewer apoptotic cells were detectable in Neo vector-transfected cells (Fig. 2B, top). To further confirm the role of TAp73 β on paclitaxel-induced apoptosis, cells were transfected with TAp73 β small interfering RNA (siRNA) and then treated with paclitaxel. TAp73 β siRNA completely abolished TAp73 β induction (Fig. 2C), DNA fragmentation (Fig. 2D), and TUNEL-positive apoptotic cells (Fig. 2E) by paclitaxel. In addition, normally residing within the cytosol, Bax levels were significantly reduced within cytosolic fractions by paclitaxel treatment and increased in the mitochondrial fraction, but significantly attenuated in TAp73 β siRNA-transfected cells. Similarly, cytochrome *c* release from the mitochondria into the cytosol was significantly attenuated by TAp73 β siRNA (Fig. 2F). These results suggest that in p53-inactivated cervical cancer

HeLa cells, TAp73 β induced by paclitaxel plays an essential role in the induction of apoptosis.

TAp73 β Induces Apoptosis via a p53-Independent Pathway

To confirm whether TAp73 β plays an essential role in paclitaxel-induced apoptosis via a p53-independent pathway, we performed similar experiments using transfection of p53 siRNA into human breast carcinoma MCF-7 cells, which contains both wild-type p53 and TAp73. As shown in Fig. 3A, p53, which increased significantly in response to paclitaxel treatment were almost completely abolished by p53 depletion in MCF-7 cells, whereas Bax and p21 expression as well as TAp73 β induced by paclitaxel were not strongly altered by p53 siRNA transfection, indicating that paclitaxel-induced apoptosis may be regulated in a TAp73 β -dependent pathway, not in a p53-dependent pathway. As expected, paclitaxel-induced TAp73 β overexpression and apoptosis was observed concomitantly in both control and p53 siRNA-transfected MCF-7 cells (Fig. 3B). In order to further confirm that paclitaxel-induced apoptosis is mediated by TAp73, not by a p53-independent pathway, we took advantage of

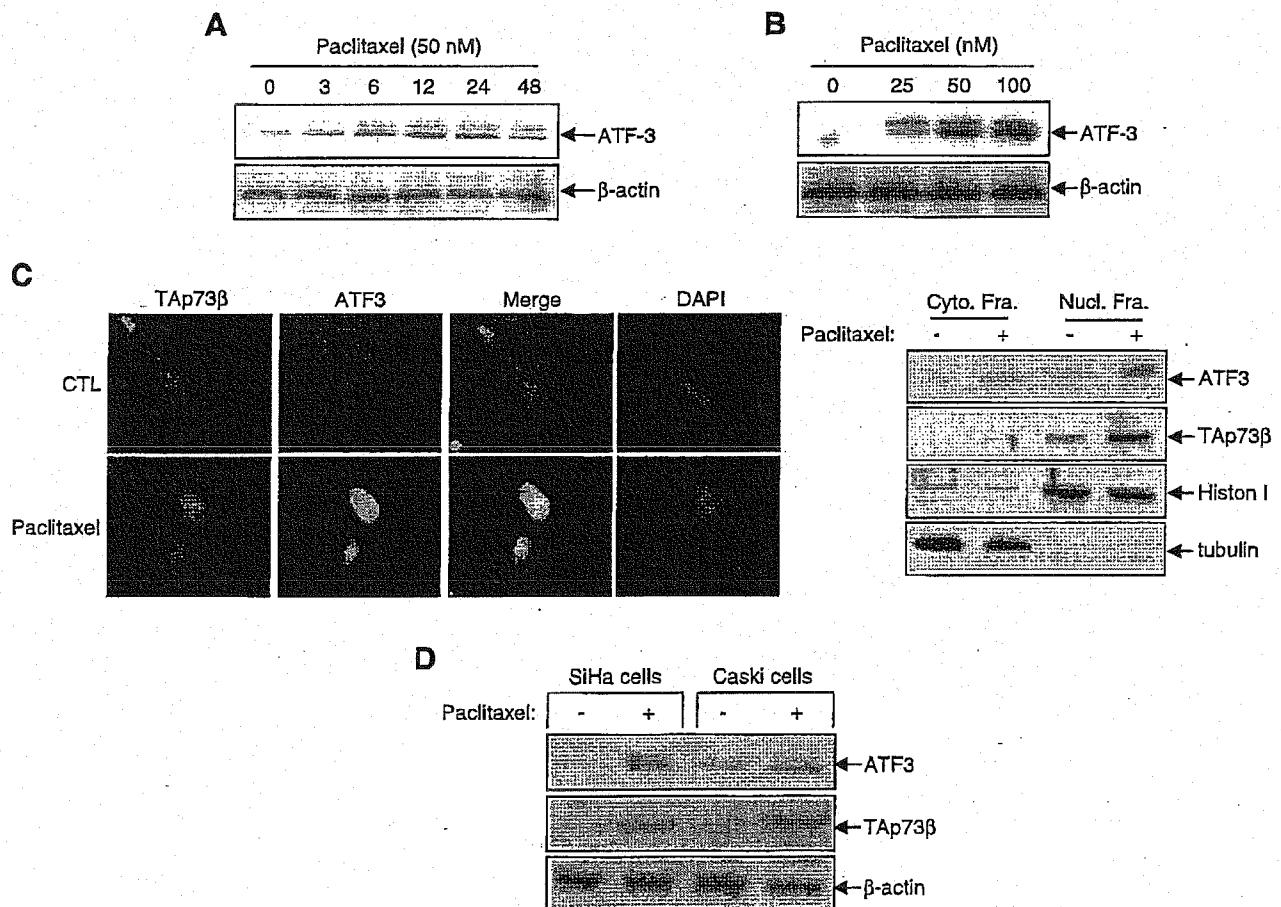
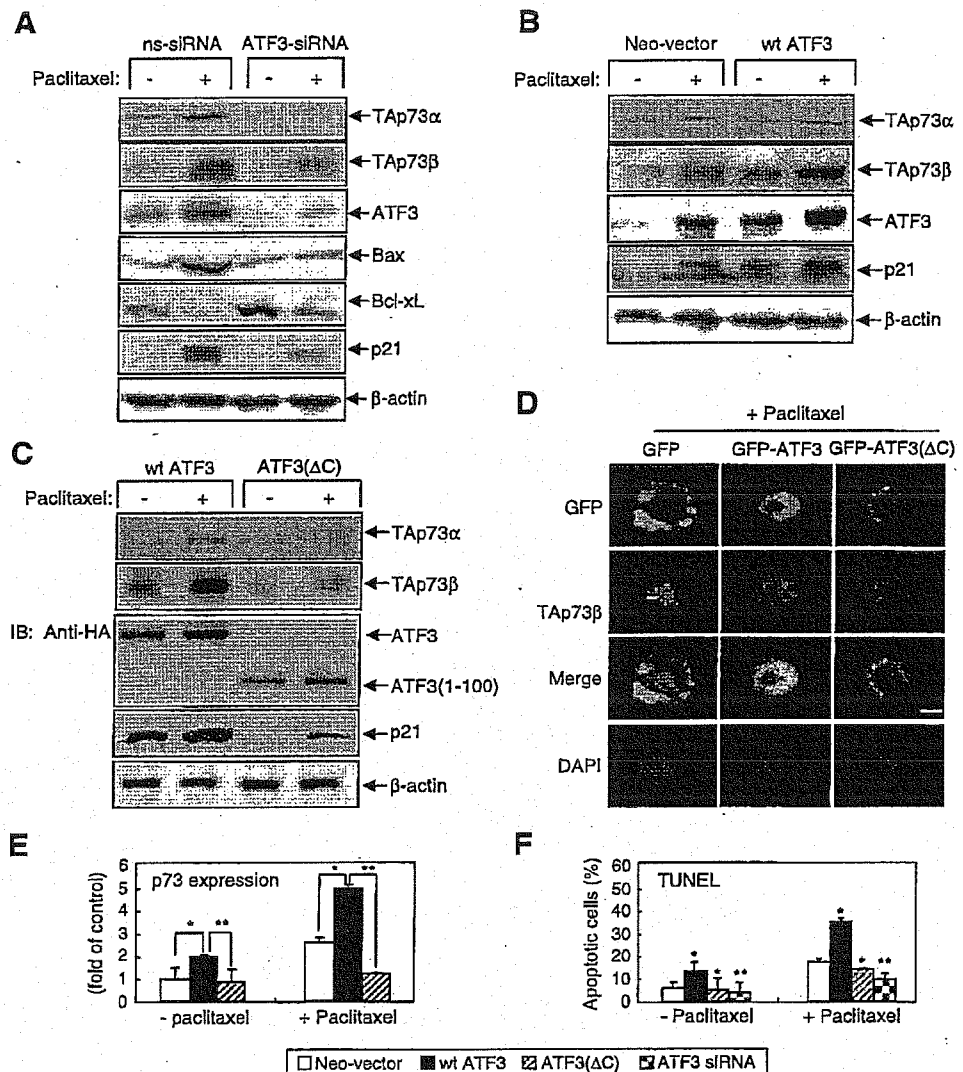


FIGURE 4. The effects of paclitaxel on ATF3 expression. **A** and **B.** Expression of ATF3 proteins. HeLa cells were treated with paclitaxel for the indicated time points (**A**) and at the different concentrations (**B**). **C.** Immunocytochemistry for TAp73 β and ATF3 and 4',6-diamidino-2-phenylindole (DAPI) staining. Fluorescent microscopic images were taken for TAp73, ATF3, and the final merged images and 4',6-diamidino-2-phenylindole nuclear staining are shown (bar, 10 μ m). **D.** Expression of ATF3 and TAp73 β in SiHa and Caski cells.

FIGURE 5. The effects of ATF3 overexpression on paclitaxel-induced TAp73 expression and apoptosis. **A.** HeLa cells were transfected with ATF3 siRNA and then treated with paclitaxel. Whole-cell lysates were subjected to Western blotting using specific antibodies. **B.** Effects of wild-type ATF3 on paclitaxel-induced apoptotic proteins. **C.** HeLa cells were transfected with the expression vector encoding for wild-type ATF3 and COOH terminal-deleted ATF3, ATF3(Δ C). After transfection for 48 h, cells were treated with paclitaxel and analyzed by Western blot against anti-TAp73 α , TAp73 β , anti-HA (for ATF3), and anti-p21 antibodies. **D** and **E.** After transfection with empty GFP, GFP-ATF3, or GFP-ATF3(Δ C), cells were treated with paclitaxel and fixed. Fluorescent microscopic images were taken for GFP (for ATF3), TAp73 β , and the final merged images and 4',6-diamidino-2-phenylindole staining (**D**) were shown (top; bar, 10 μ m) and quantified (**E**). **F.** TUNEL-positive apoptotic cells. Columns, average from three independent experiments; bars, SE (*, $P < 0.05$; **, $P < 0.01$).



p53-null human osteosarcoma SAOS2 cell lines, which are p53-deficient and do not express TAp73 at the mRNA or protein levels. Moreover, the SAOS2 cell line may be a particularly suitable *in vitro* model for evaluating the role of TAp73 on paclitaxel-induced apoptosis, as it is well known that paclitaxel induces TAp73 expression in these cells (29). As shown in Fig. 3C, although p53 protein expression was undetectable in paclitaxel-treated SAOS2 cells, the expression levels of TAp73 β , Bax, and p21 increased following treatment with paclitaxel in both MCF-7 and SAOS2 cells. Additionally, the levels of TAp73 β expression and TUNEL-positive apoptotic cells increased by paclitaxel, as observed in SAOS2 cells, was even lower than the increase observed in MCF-7 cells (Fig. 3D).

ATF3 Potentiates TAp73 β -Mediated Apoptosis in Paclitaxel-Treated HeLa Cells

Our data show that paclitaxel-induced apoptosis was regulated in a TAp73-dependent and p53-independent pathway;

however, the upstream regulator involved in TAp73 overexpression is still not clear. To elucidate the mechanism by which TAp73 expression is up-regulated, we screened for changes in the expression profile of several transcription factors after treatment with paclitaxel (data not shown). The results showed that paclitaxel significantly increased the expression of the stress-inducible gene, ATF3, in a time-dependent and dose-dependent manner (Fig. 4A and B), which was concomitantly increased with TAp73 α and TAp73 β expression (Fig. 1D). In addition, most of the ATF3 induced by paclitaxel was colocalized with TAp73 β in the nucleus, although this was not significant in control cells (Fig. 4C, left), which was confirmed by data showing that ATF3 and TAp73 β levels were concomitantly increased within the nuclei fractions following paclitaxel treatment (right). This finding suggested that paclitaxel-induced ATF3 might be involved in increasing TAp73 β up-regulation to compensate for the apoptotic roles of p53 in p53-inactivated HeLa cells. Because HeLa cells are

HPV-18-positive cell lines, we have examined whether paclitaxel induced ATF3 and TAp73 β in other HPV-positive cell lines such as SiHa and Caski cells, which were positive for HPV-16 (Fig. 4D). As expected, paclitaxel abundantly induced ATF3 and TAp73 β in both cells, indicating that the inductions of ATF3 and TAp73 β by paclitaxel were not specific for the strains of HPV.

Next, to define the direct role of ATF3 on paclitaxel-induced TAp73 β expression and apoptosis, HeLa cells were transiently transfected with ATF3 siRNA and then treated with paclitaxel. The expression of TAp73 α , TAp73 β , Bax, and p21 increased by paclitaxel were attenuated significantly by ATF3 depletion.

Also, ATF3 siRNA attenuated paclitaxel-mediated down-regulation of Bcl-xL expression (Fig. 5A). Paclitaxel-induced TAp73 and its downstream target p21 and Bax were potentiated by wild-type ATF3 overexpression, which were significantly decreased in cells transfected with ATF3(Δ C), a deletion in the COOH-terminal (101-181) region was necessary for interaction with other proteins (30).

As a transcriptional factor, nuclear localization of ATF3 is likely a prerequisite for its activity. Therefore, we next examined whether paclitaxel-induced apoptosis is mediated by the direct effects of ATF3 on p73 activation and localization into the nucleus. As shown in Fig. 5D and E, paclitaxel-induced

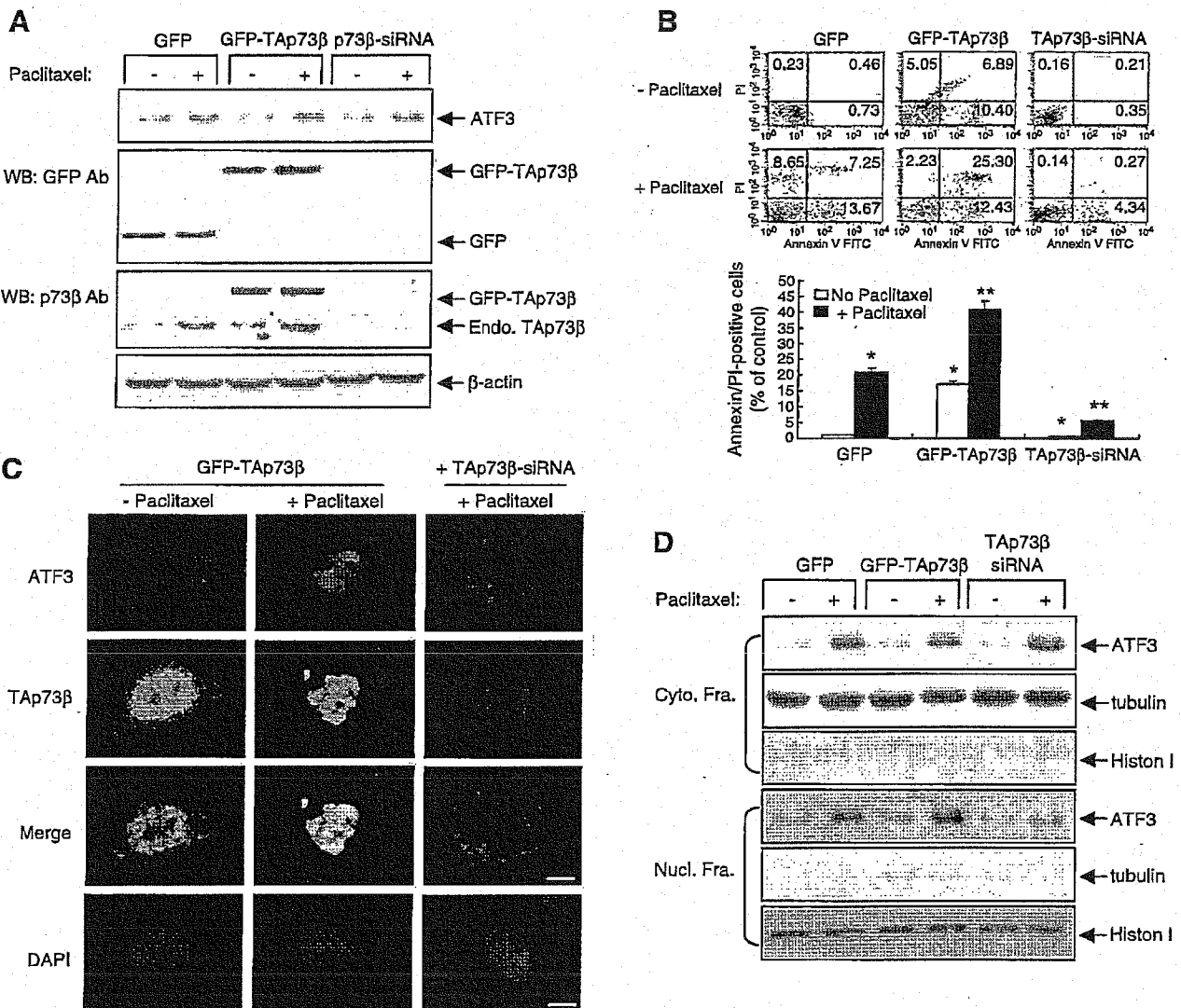
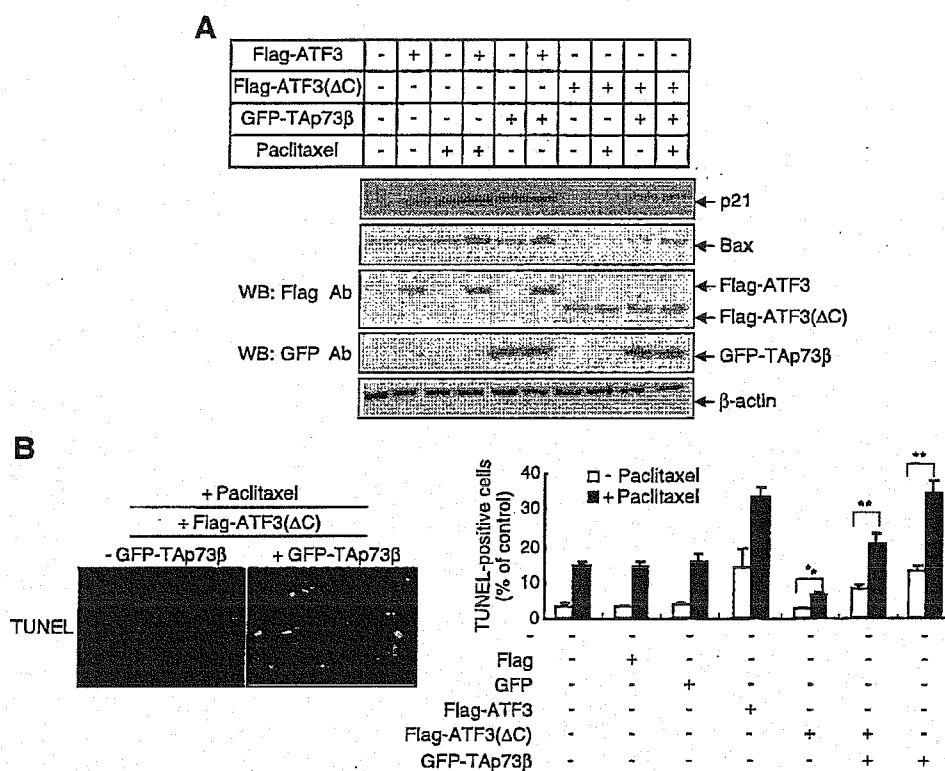


FIGURE 6. The effects of TAp73 β or TAp73 β siRNA overexpression on paclitaxel-induced apoptosis. **A.** Effects of TAp73 β overexpression on ATF3 induced by paclitaxel. The cells were transfected with GFP-TAp73 β alone or TAp73 siRNA, and then treated with paclitaxel. The cell lysates were subjected to Western blotting using anti-ATF3, anti-GFP, anti-TAp73 β antibodies. **B.** TAp73 β depletion inhibits the potentiation of TAp73 β on paclitaxel-induced apoptosis. After transfection with GFP-empty vector, GFP-TAp73 β , or TAp73 β siRNA, cells were incubated with Annexin V and propidium iodide, and analyzed for cell apoptosis by fluorescence-activated cell sorting analysis (top) and quantified (bottom). **C.** Effects of TAp73 β depletion using TAp73 β siRNA on paclitaxel-induced ATF3 expression. Cells transfected with GFP-TAp73 β or TAp73 β siRNA were treated with paclitaxel and fixed. Fluorescent microscopic images were taken for GFP (for TAp73 β), ATF3, and the final merged images were shown (top; bar, 10 μ m). **D.** TAp73 β depletion prevents ATF3 translocation into the nuclear fraction induced by paclitaxel.

FIGURE 7. The effects of ATF3 or ATF3(Δ C) on paclitaxel-induced apoptosis. **A.** HeLa cells were cotransfected with flag-tagged ATF3 or ATF3(Δ C) in the presence or absence of GFP-p73 β and then treated with paclitaxel. Whole-cell lysates were subjected to Western blotting against anti-p21, anti-Bax, anti-Flag, and anti-GFP antibodies (*top*) and quantified (*bottom*). **B.** Flag-tagged ATF3(Δ C) inhibits the potentiation of p73 β on paclitaxel-induced apoptosis. TUNEL assay (*top*) and TUNEL-positive apoptotic cells were quantified (*bottom*). Columns, average from three independent experiments; bars, SE (*, $P < 0.05$; **, $P < 0.01$).



TAp73 β expression was increased significantly by GFP-ATF3 overexpression, whereas GFP-ATF3(Δ C)-transfected cells resulted in minor increases (Fig. 5D and E, *left*). Interestingly, most of the GFP-ATF3 activated by paclitaxel translocated into the nucleus, but GFP-ATF3(Δ C) was primarily found around the nucleus (Fig. 5D). Furthermore, it seems that the degree of apoptosis induced by paclitaxel was different based on the location of ATF3. Levels of TUNEL-positive apoptotic cells increased in GFP-ATF3-transfected cells, but decreased significantly in ATF3(Δ C)-transfected cells. These results are also supported by using ATF3 siRNA. Apoptosis increased by paclitaxel or ATF3 overexpression was significantly decreased in ATF3 siRNA, such as that in ATF3(Δ C)-transfected cells (Fig. 5F). These results suggest that ATF3, especially the COOH-terminal region (101-181) of ATF3, may play an important role in the functionality of TAp73 and may function as an upstream regulator of TAp73 induced by paclitaxel treatment. We have also observed similar results in other cervical cancer cell lines (Caski and SiHa cells; see Supplementary Data).

Depletion of TAp73 β Affects ATF3 Localization, but not ATF3 Expression in Paclitaxel-Treated HeLa Cells

Our data showed that in HeLa cells, ATF3 strongly augmented TAp73 β up-regulation induced by paclitaxel, resulting in apoptosis, but we couldn't exclude the possibility that TAp73 β can reversibly affect ATF3 expression or activation. Therefore, after transfection of GFP-TAp73 β or TAp73 β siRNA, we examined whether TAp73 β overexpression affects ATF3 expression and nuclear translocation induced by paclitaxel. As shown in Fig. 6A, paclitaxel treatment increased

ATF3 expression in GFP-empty vector-transfected cells, but paclitaxel-induced ATF3 expression was unaffected by GFP-TAp73 β overexpression. Additionally, paclitaxel-induced ATF3 expression was not changed by TAp73 β depletion in TAp73 β siRNA-transfected cells. This finding further supports previous data that ATF3 is an upstream regulator of TAp73 β induced by paclitaxel. We have also observed similar results in other cervical cancer cell lines (Caski and SiHa cells; see Supplementary Data). However, it may be possible that TAp73 β plays an essential role in apoptosis induced by paclitaxel-activated ATF3 because compared with GFP-transfected cells, paclitaxel strongly enhanced GFP-TAp73 β -induced apoptosis, which was significantly attenuated by the depletion of TAp73 β (Fig. 6B). GFP-TAp73 β alone also induced early-stage apoptosis (*bottom right*), whereas cotreatment of paclitaxel in GFP-TAp73 β -transfected cells increased Annexin V-propidium iodide double staining cells (late-stage apoptosis). As the data showed that decreased ATF3(Δ C) translocation into the nucleus resulted in reduced paclitaxel-mediated apoptosis through lowered TAp73 β expression (Fig. 5D and E), we examined whether TAp73 β depletion affected paclitaxel-induced apoptosis by altering ATF3 translocation into the nucleus (Fig. 6C). In GFP-TAp73 β -overexpressing cells, ATF3 expression was potentiated by paclitaxel and colocalized with GFP-TAp73 β in the nucleus. Meanwhile, nuclear translocation of ATF3 significantly decreased in TAp73 β siRNA-transfected cells and ATF3 located primarily around the nucleus, correlating with reduced TAp73 β expression. These results suggest that functional TAp73 β may be needed for ATF3 activation and its translocation into the nucleus, although TAp73 β did not affect

ATF3 expression. To define this possibility, the expression of ATF3 in the isolated cytosolic or nuclear fraction was examined (Fig. 6D). Paclitaxel-enhanced ATF3 expression was observed in both the cytosol and nuclear fractions of GFP- or GFP-TAp73 β -transfected cells, whereas ATF3 in TAp73 β siRNA-transfected cells was detected mostly in the cytosolic fraction, and weakly in the nuclear fraction, indicating that TAp73 β may play an important role in inducing ATF3 activation and nuclear translocation. Tubulin (cytoplasmic protein) and histone I (nuclear protein) were used to confirm whether cytosolic and nuclear fractions were isolated purely from cell extracts.

TAp73 β Plays an Essential Role in ATF3-Mediated Apoptosis

To examine the effect of ATF3 on paclitaxel-induced apoptosis, HeLa cells were cotransfected with flag-tagged ATF3 or ATF3(Δ C) in the presence or absence of GFP-TAp73 β

and then treated with paclitaxel. First, ATF3 overexpression increased the expression of p21 and Bax, TAp73 downstream target proteins related to apoptosis, which was potentiated by paclitaxel (Fig. 7A). In contrast, p21 and Bax were not increased by paclitaxel cotreatment in flag-ATF3(Δ C)-overexpressed cells, indicating that ATF3 was required for the induction of p21 and Bax by paclitaxel. Interestingly, weak expression of Bax and p21 in ATF3(Δ C)-transfected cells was strongly recovered in GFP-TAp73 β -transfected cells, which was potentiated by paclitaxel treatment. In addition, paclitaxel-induced apoptosis increased strongly in Flag-ATF3-transfected cells, but was observed to be weak in Flag-ATF3(Δ C)-transfected cells (Fig. 7B). However, inhibition of apoptosis in ATF3(Δ C)-transfected cells was recovered in part, but not completely, in cells cotransfected with GFP-TAp73 β (Fig. 7B, left). Although paclitaxel did not increase apoptosis in ATF3(Δ C)-transfected cells, overexpression of GFP-TAp73 β alone restored apoptosis

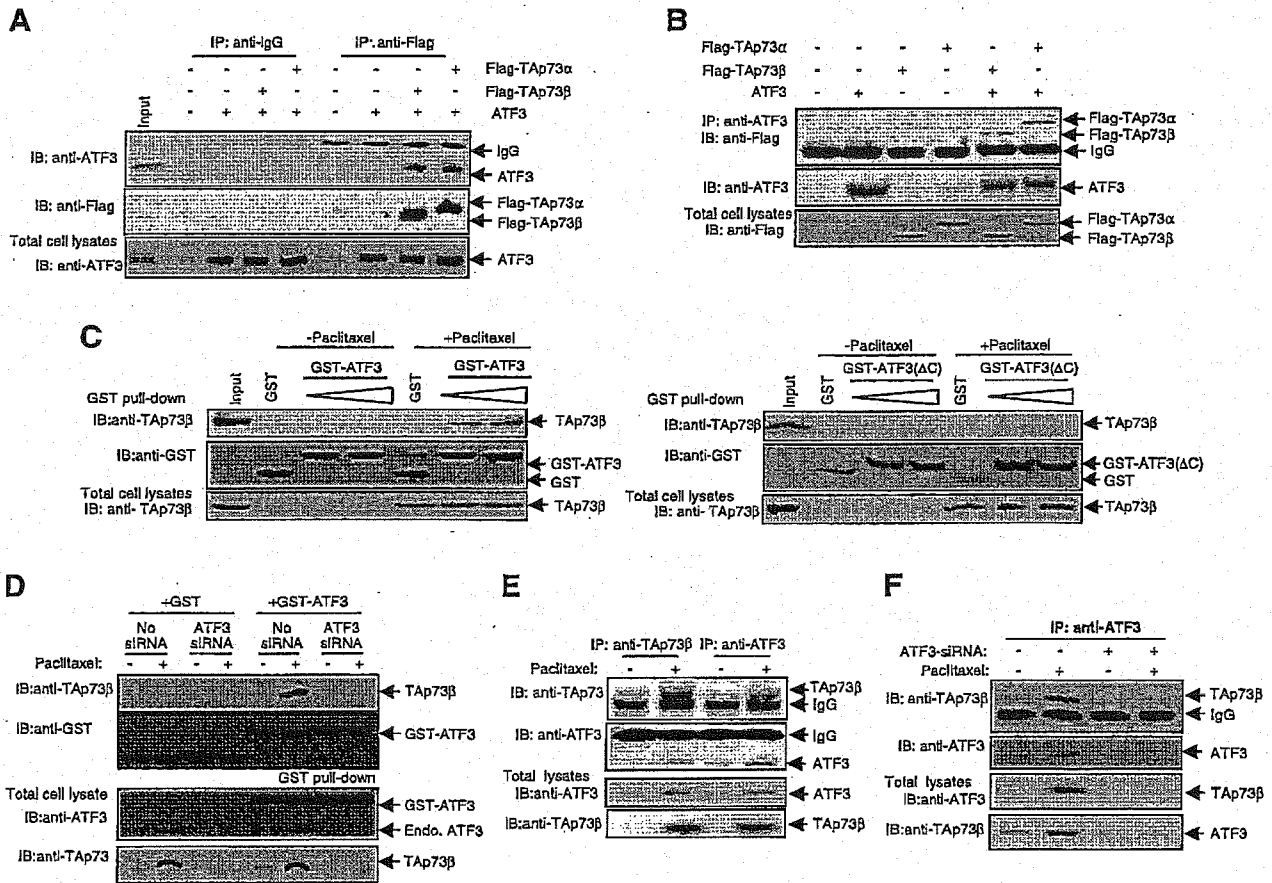


FIGURE 8. Interaction of ATF3 with TAp73 β in paclitaxel-treated HeLa cells. HeLa cells were cotransfected with ATF3 in the absence or presence of flag-tagged TAp73 α or TAp73 β . **A.** After transfection, cell lysates were immunoprecipitated (IP) with anti-IgG or anti-flag (for TAp73 β) and then immunoblotted (IB) using anti-ATF3 and anti-flag antibodies. Total lysates were immunoblotted with anti-ATF3 and anti-TAp73 β . **B.** Cell lysates were immunoprecipitated (IP) with anti-ATF3 and then immunoblotted (IB) using anti-flag and anti-ATF3. Total lysates were immunoblotted with the anti-flag. **C.** *In vitro* binding assay using GST pull-down assay and purified GST, GST-ATF3 (top), or GST-ATF3(Δ C) was mixed with paclitaxel-treated cell lysates and subjected to SDS-PAGE, and immunoblotted with anti-TAp73 β and anti-GST. Total cell lysates were also immunoblotted with anti-TAp73 β antibody. **D.** ATF3 depletion inhibits the endogenous TAp73 β expression and their *in vitro* binding. HeLa cells were transfected with ATF3 siRNA, then treated with paclitaxel. Cell lysates were incubated with GST or GST-ATF3 and then analyzed by GST pull-down assay. *In vivo* binding assay (**E**) and ATF3 depletion (**F**) inhibits *in vivo* binding. After treatment with paclitaxel in the absence (**E**) or presence (**F**) of ATF3 siRNA, the immunoprecipitated lysates with anti-p73 (left) or anti-ATF3 (right) were subjected to immunoblotting with anti-TAp73 β and anti-ATF3 antibodies. Total cell lysates were also immunoblotted with anti-ATF3 and anti-TAp73

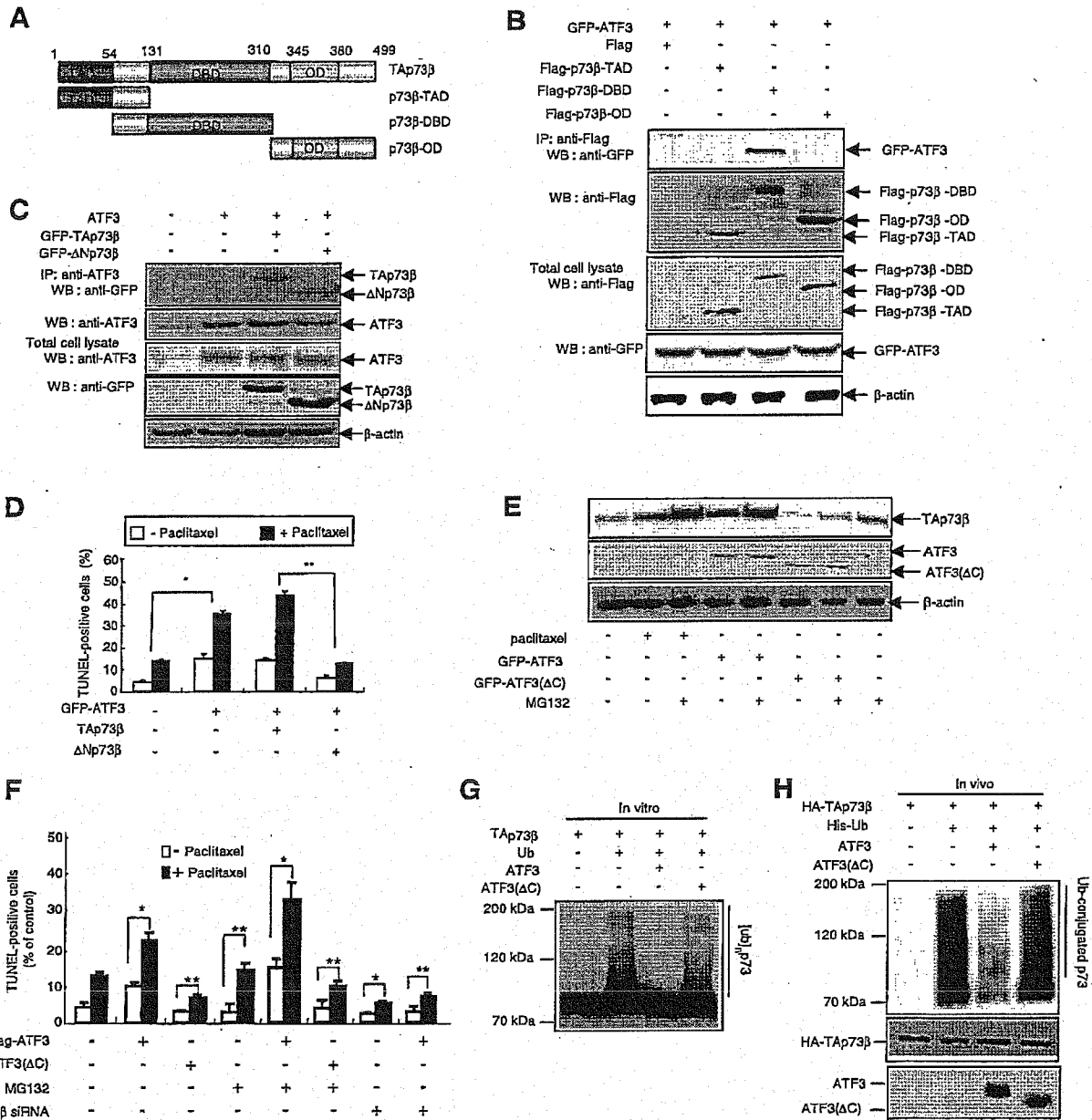


FIGURE 9. Identification of specific binding regions of TAp73β interacted with ATF3. **A.** Diagrams of p73β divided according to specific domains [transactivation (TAD), DNA-binding (DBD), and oligomerization (OD) domains]. Flagged-tagged cDNAs containing each of the domains were constructed. **B.** After transfecting each of the flag-tagged truncated forms of p73β together with GFP-ATF3 into the cells, the cell lysates were immunoprecipitated with anti-flag antibody, and the samples were assessed by immunoblot analysis using anti-GFP and anti-flag antibody (left). Total cell lysates were also immunoblotted with anti-flag and anti-GFP antibodies (right). **C.** Interaction of ATF3 with GFP-TAp73β or ΔNp73β. **D.** Effects of GFP-TAp73β or ΔNp73β on paclitaxel-induced apoptosis (TUNEL assay). Columns, average from three independent experiments; bars, SE (*, $P < 0.05$; **, $P < 0.01$; bottom). **E.** Effects of ATF3 on TAp73β stability induced by paclitaxel. Cells were transfected with GFP-ATF3 or GFP-ATF3(ΔC) and then treated with MG132, a proteasome inhibitor. Whole-cell lysates were subjected to Western blotting using anti-TAp73β and anti-GFP (for ATF3) antibodies. **F.** Effects of ATF3-mediated TAp73β stabilization on paclitaxel-induced apoptosis (TUNEL assay). Columns, average from three independent experiments; bars, SE (*, $P < 0.05$; **, $P < 0.01$; bottom). **G.** *In vitro* ubiquitination assay. GST-TAp73β protein was preincubated with 250 ng of the full-length or the deleted mutant ATF3 protein and then subjected to Western blotting for ubiquitinated TAp73β using anti-polyubiquitin antibody (FK-1). **H.** ATF3 inhibits the ubiquitination of TAp73β *in vivo*. Cells were transiently cotransfected with the indicated combinations of expression plasmids and treated with MG132. Ubiquitinated products were recovered on nickel-agarose beads and separated by SDS-PAGE, followed by immunoblotting with anti-HA antibody.

similar to apoptosis induced by paclitaxel in control cells (Fig. 7B, right), suggesting that TAp73β is an important downstream regulator of ATF3-mediated apoptosis and is required for ATF3-mediated apoptosis.

ATF3 Directly Binds TAp73β in Paclitaxel-Treated Cells

Previously, TAp73 homologous p53 protein levels were elevated by stress via an increased stability and its protein stability could be regulated by associated proteins (25). Because

not found to interact with ATF3 and Flag-TAp73 α or TAp73 β (Fig. 8A, *left*), indicating that TAp73 interacts specifically with ATF3 *in vivo*. The total cell lysates were also determined by Western blotting using ATF3 and flag antibodies (*bottom*). To corroborate whether ATF3 directly binds endogenous TAp73 β , cells were treated with paclitaxel to simulate conditions that stimulate TAp73 expression, and subsequently, the GST pull-down assay was conducted using purified GST, GST-fused ATF3, or GST-ATF3(Δ C). From here, we examined the interaction of ATF3 with TAp73 β because this interaction is higher than that with TAp73 α . As shown in Fig. 8C, association of TAp73 β with GST-ATF3 (*left*) observed in paclitaxel-treated cells (*lanes 6 and 7*), but not in control cells (*lanes 3 and 4*). The association of GST-ATF3 with TAp73 β might be due to the increase of TAp73 β induced endogenously by paclitaxel because the association was not detected in control cells, and did not express TAp73 β . However, GST-ATF3(Δ C) (*right*) or control GST beads did not associate with TAp73 β , although TAp73 β was induced in paclitaxel-treated cells (*lanes 5-7*), suggesting that TAp73 β induced endogenously by paclitaxel interacts directly with ATF3, specifically, with the COOH-terminal region. Next, we examined whether ATF3 depletion using ATF3 siRNA affects the association of GST-ATF3 with endogenous TAp73 β induced by paclitaxel. As shown in Fig. 8D, the interaction between GST-ATF3 and TAp73 β was detected in paclitaxel-treated cells (*lanes 5 and 6*), which was abolished completely in ATF3 siRNA-transfected cells (*lanes 7 and 8*), and correlated with the reduction in p73 β expression through the silencing of endogenous ATF3 (*bottom, lanes 7 and 8*). In contrast, TAp73 β induced by paclitaxel was not associated with control GST (*lanes 1 and 2*). These results suggest that ATF3 may be involved in stabilizing TAp73 β protein induced by paclitaxel treatment and affects the association between them. Next, we have examined whether endogenous ATF3 and TAp73 β induced by paclitaxel could also interact with each other *in vivo*. As expected, after paclitaxel treatment, both endogenous TAp73 β and ATF3 were immunoprecipitated together, which was correlated with the proportional increase of ATF3 and TAp73 β by paclitaxel treatment (Fig. 8E). However, an increase of endogenous TAp73 β captured by immunoprecipitated ATF3 was also completely abrogated by ATF3 siRNA transfection, which correlated with decreased levels of TAp73 β via ATF3 depletion (Fig. 8F). We therefore suggest that stabilization of TAp73 β by ATF3 may be due to the increased steady-state levels of these proteins or the interaction of these two proteins.

ATF3 Interacts with the DNA-Binding Domain of TAp73 β and Stabilizes the TAp73 β

Next, to determine the binding region of TAp73 β that is necessary for interactions with ATF3, we constructed a series of truncated mutants that contained distinct domains of TAp73 β (Fig. 9A). After cotransfection of the p73 β -transactivation domain, p73 β DNA-binding domain, and p73 β -oligomerization domain mutants with GFP-ATF3 into HeLa cells, overexpressing mutant flag-p73 β s were immunoprecipitated with anti-flag antibody, and the immunoprecipitates were Western blotted using anti-GFP antibody to detect ATF3 (Fig. 9B). Neither the p73 β -transactivation domain nor the p73 β -

oligomerization domain regions seemed to interact with ATF3, whereas the p73 β DNA-binding domain-containing region (amino acids 54-310) strongly interacted with ATF3, indicating that the DNA-binding domain region of p73 β is responsible for the interaction with ATF3. In general, unlike p53, p73 generate two major protein isoforms, transactivation and Δ N domains, through two different promoters and three alternative splicing sites at the 3' end, denoted by α , β , γ (9). Furthermore, the transactivated isoform of p73 acts more like p53, whereas the Δ N isoform shows a dominant-negative function to TAp73 isoforms (31). Therefore, we have examined whether ATF3 interacts with dominant negative Δ Np73 β similar with TAp73 β and thus affects paclitaxel-induced apoptosis. As shown in Fig. 9C, immunoprecipitated ATF3 interacts with Δ Np73 β similar with TAp73 β . However, TAp73 β cotransfection, but not Δ Np73 cotransfection, highly induced apoptosis, which was potentiated by paclitaxel (Fig. 9D), suggesting that Δ Np73 β could be opposing effects on apoptosis mediated by TAp73 β , although ATF3 interacts with the DNA-binding domain of p73 β .

Similar to p53, mdm2 binds to TAp73 and inhibits TAp73-mediated transcriptional activation and apoptosis; however, mdm2 failed to ubiquitinate TAp73 (32). Furthermore, it was reported that ATF3 interacts with p53 and prevents the ubiquitination and degradation of the latter, and consequently, augmenting p53 function (18, 29). Therefore, to investigate whether paclitaxel-induced ATF3 also mediates TAp73 β expression and function by preventing ubiquitination and degradation, cells were pretreated with MG132, a proteasome inhibitor, in wild-type ATF3 or ATF3(Δ C)-overexpressing cells (Fig. 9E). Pretreatment with MG132 for 2 hours significantly enhanced TAp73 β expression induced by paclitaxel (*lane 3*). TAp73 β expression increased in cells overexpressing ATF3 alone, which was potentiated by MG132 pretreatment (*lanes 4 and 5*), but not ATF3(Δ C)-overexpressing cells (*lane 6*). The TAp73 β protein levels were increased slightly by MG132 in ATF3(Δ C)-overexpressing cells (*lane 7*) and even by itself MG132 (*lane 8*). Similar to this, MG132 significantly enhanced paclitaxel-induced apoptosis, which was potentiated by ATF3 overexpression, but not by ATF3(Δ C)-overexpression. TUNEL-positive apoptotic cells induced by ATF3 overexpression were also almost completely decreased by TAp73 β siRNA, indicating that ATF3-induced apoptosis is due to the induction of TAp73 β (Fig. 9F). Next, to examine the direct effects of ATF3 on the ubiquitination of TAp73 β , we did an *in vitro* ubiquitination assay by using an *in vitro*-reconstituted ubiquitination reaction system with E1, E2 enzymes, and GST-ATF3 or GST-ATF3(Δ C) recombinant proteins (Fig. 9G). In the presence of all the required ubiquitination reaction components, the addition of recombinant ATF3 protein completely reduced TAp73 β ubiquitination. Unlike the full-length protein, the ATF3 protein in which the COOH-terminal domain is deleted, preventing it from binding with TAp73 β , was less effective in blocking TAp73 β ubiquitination *in vitro*. We have determined if ATF3 could also inhibit the ubiquitination of TAp73 *in vivo*, HeLa cells were transiently cotransfected with the expression plasmids for HA-TAp73 β and His-ubiquitin with plasmid for ATF3 or ATF3(Δ C). Forty-eight hours after transfection, whole-cell lysates were prepared

and analyzed by immunoblotting for the presence of His-ubiquitin-containing TAp73 β . As shown in Fig. 9H, the amounts of ubiquitinated TAp73 β were decreased in the presence of ATF3, whereas ATF3(Δ C) inhibited the ubiquitination of TAp73 β to a lesser degree. Altogether, these results strongly suggest that binding of TAp73 β to the COOH-terminal region of ATF3 inhibits the ubiquitination of TAp73 β , thereby increasing the stability of TAp73 β .

ATF3 Potentiates the Transactivation of TAp73 Target Promoters

Because transcriptional regulation of the TAp73 gene contributes to its activation in response to various stress stimuli (10, 33) and our data showed that paclitaxel-induced ATF3 might be involved in TAp73 up-regulation, we also hypothesized that ATF3-dependent induction of TAp73 is regulated by enhancement of TAp73 transcriptional levels. However, increased TAp73 protein accumulation by paclitaxel-induced ATF3 was not due to transcriptional regulation because TAp73 mRNA levels did not change in response to paclitaxel treatment at different times (Fig. 10A), which may be due to the induction of mitotic arrest, leading to the absence of transcription. Therefore, to examine whether ATF3 can regulate newly synthesized TAp73 β proteins, cells transfected with TAp73 β in the absence or presence of ATF3 were treated with cycloheximide, an inhibitor of *de novo* protein synthesis, for the indicated time points. TAp73 β levels were significantly decreased after 3 hours of cycloheximide treatment, which was attenuated significantly by ATF3 overexpression (Fig. 10B, *top*). Paclitaxel-induced endogenous TAp73 β levels were also significantly decreased by cycloheximide in Neo vector-overexpressed cells, which was attenuated in ATF3-overexpressed cells (*bottom*), suggesting that ATF3 regulates the accumulation of paclitaxel-induced TAp73 β by enhancing protein stability.

Next, to define the possibility that ATF3 could also affect TAp73 β -dependent transcriptional activation, HeLa cells were transiently transfected with the TAp73 β cDNA and a luciferase reporter containing the TAp73-responsive element from p21 or Bax promoters, together with ATF3 or ATF3(Δ C) expression plasmids and then treated with paclitaxel. As shown in Fig. 10C, ATF3 potentiated paclitaxel-induced p21- or Bax-luciferase activities, but was attenuated by cotransfection with ATF3(Δ C). In addition, TAp73 β -induced p21- or Bax-luciferase activities increased significantly in ATF3-cotransfected cells, which were not found in ATF3(Δ C)-transfected cells. The silencing of ATF3 by ATF3 siRNA strongly inhibited ATF3-induced p21- or Bax-luciferase activation. TAp73 β siRNA also inhibited TAp73 β -induced p21 and Bax transcriptional activity (Fig. 10D). These data suggest that paclitaxel-induced ATF3 mediates TAp73 β transactivation, followed by p21 and Bax gene transcription. Thus, to examine whether ATF3 can mediate direct interactions between the TAp73 β and p21 promoter, electrophoretic mobility shift assays were done using nuclear extracts from paclitaxel-treated, ATF3-transfected or TAp73 β -transfected cells (Fig. 10E). For these experiments, 42-bp oligonucleotides were designed that span the putative TAp73-binding site containing the sequence of the TAp73 response element in the p21 promoter. As shown in Fig. 10E, paclitaxel

increased the TAp73 β -p21 binding complex, which was further potentiated by cotransfection of ATF3, but was completely abolished by 100-fold excess of unlabeled oligonucleotides. In addition, the complexes increased by ATF3 and TAp73 β transfection were completely abrogated by ATF3 siRNA and TAp73 siRNA, respectively. To ascertain whether the complex consisted of bound TAp73, a supershift assay was conducted with the antibody against TAp73 and ATF3. Results show that both anti-TAp73 and anti-ATF3 shifted the binding complex, although the shifted locations were different. In contrast, no supershifted complex was detected with anti-STAT5 antibody, which was used as a negative control (Fig. 10F). Thus, it is likely that ATF3 potentiated the direct interaction of TAp73 to the TAp73-binding site located in the p21 promoter, increasing TAp73's transcriptional activity. Next, to clarify the precise molecular mechanism by which ATF3 mediates the transcriptional activity of TAp73 on p21 or Bax promoter, we did a chromatin immunoprecipitation analysis. Cross-linked chromatin prepared from HeLa cells transiently transfected with GFP-empty or GFP-ATF3 plasmids were treated with paclitaxel and immunoprecipitated with the indicated antibodies, followed by amplification with the indicated promoter-specific primers. As shown in Fig. 10G, TAp73 β and ATF3 were efficiently recruited to the p21 and Bax promoters in control cells, which were increased strongly in paclitaxel-treated cells. Furthermore, a significant increase in chromatin binding was higher in the presence of ATF3 than in cells transfected with GFP alone. This observation correlates with our previous finding that ATF3 enhanced the transcriptional activity of TAp73 β . Interestingly, ATF3 also binds to the TAp73 β binding sites on p21 or Bax promoters. This recruitment of ATF3 to TAp73 β binding sites was specific because we did not observe any amplification in STAT5 immunoprecipitated chromatin. These data suggest that ATF3 might directly bind to TAp73 β binding sites or play as a cofactor mediating p73 functional activity.

Discussion

In this study, we showed that a novel transcription factor, ATF3, interacts directly with TAp73 and enhances the stability of the latter, thereby acting as a tumor-inhibiting factor through stimulating apoptosis mediated by TAp73 after induction by paclitaxel. Paclitaxel is a broad-spectrum anticancer agent which is currently used in treating many types of advanced cancer including cervical, breast, and ovarian cancers, although resistance to paclitaxel chemotherapy occurs in some patients with cancer (8, 34). The primary antitumor mechanism of action by paclitaxel is through its ability to bind to microtubules and prevent their assembly, causing cells to arrest in G₂-M, and consequently, resulting in apoptotic cell death (4, 5). Several studies have been reported in which paclitaxel induces apoptosis through nuclear factor κ B down-regulation and Akt phosphorylation followed by mTOR activation, a downstream target of Akt (35). However, the role of paclitaxel in regulating cell death in various cancer cells, including cervical cancer cells, has been extensively studied, but the exact mechanisms through which paclitaxel triggers apoptosis and promotes chemocytotoxicity are still unclear.

Recently, it has been shown that TAp73-inducing agents such as cisplatin, doxorubicin, and paclitaxel could result in TAp73-mediated cell death in a p53-independent manner (16, 36). Particularly, in cervical cancer HeLa cells, two major HPV oncoproteins, E6 and E7, bind and inactivate p53 and pRb tumor suppressors for ubiquitin degradation, which impairs cell cycle control and induces apoptosis in response to DNA damage (15, 16). Despite the functional similarities between TAp73 and p53, the response against HPV E6 or HPV E7 by TAp73 is controversial. In some studies, TAp73 interacts with HPV E6 and becomes functionally inactivated, whereas in other studies, TAp73 does not interact with HPV E6 or HPV E7 and is followed by growth inhibition and apoptosis in cancer cells (37, 38). Therefore, it is important to determine whether paclitaxel could reversibly activate p53 inactivated by HPV E6 and HPV E7 oncogenes expressed in HeLa cells, and if paclitaxel could activate TAp73 to compensate for the function of inactivated p53. Our data show that paclitaxel induced TAp73 α or TAp73 β and its downstream targets, Bax and p21, but minimally induced p53 in a time-dependent manner in cervical cancer HeLa cells. Moreover, activated TAp73 enhanced p21 promoter activity and cytochrome *c* release from mitochondria, resulting in apoptosis. These effects were abrogated in cells transfected with inactive TAp73 β siRNA, and further supported by findings that TAp73 β was also induced by paclitaxel in p53-null SAOS2 cells and MCF-7 cells with depleted p53, correlating with the induction of Bax and p21 proteins and resulting in apoptosis. These results indicate that TAp73 β functions to compensate for impaired p53 function in order to trigger p53-independent apoptosis of HeLa cells in response to paclitaxel. However, we should be very cautious in drawing conclusions comparing the effects of MCF-7 and SAOS cells because these cells have very divergent genetic backgrounds. For example, MCF-7 cells lack pRb. On the other hand, paclitaxel increased the levels of antiapoptotic protein Bcl-2 expression during acute time periods (up to 24 hours), but decreased significantly 24 hours later and was sustained for up to 48 hours. Afterwards, Bcl-xL expression decreased in a time-dependent manner. The acute overexpression of Bcl-2 might be involved in the resistance to paclitaxel chemotherapy as previous studies have reported that up-regulation of Bcl-2, nuclear factor κ B, Akt, etc., may be potential signaling mediators contributing to paclitaxel resistance.

In response to stress, ATF3 interacts with p53 and enhances the stability of p53 by preventing ubiquitin degradation and augmenting p53-mediated apoptosis (25). However, contradictory evidence suggests that ATF3 inhibits doxorubicin-induced apoptosis through p53 down-regulation in cardiac myocytes (26). Therefore, we examined whether stress-inducible ATF3 activates or inactivates TAp73 function similar to p53 (Figs. 4 and 5). Our findings indicate that paclitaxel-induced TAp73 β overexpression was correlated with the induction of ATF3 and up-regulation of p21 and Bax, resulting in apoptosis. These events were augmented by the overexpression of wild-type ATF3, which was almost completely abolished by transfection with inactive ATF3 siRNA or ATF3(Δ C), a COOH-terminally deleted ATF3. Interestingly, our data also showed that activated ATF3 translocated into the nucleus, where p73 localizes, but its translocation was inhibited significantly by transfection with

ATF3 siRNA or ATF3(Δ C). Furthermore, ATF3(Δ C) overexpression significantly inhibits TAp73 α and TAp73 β expression induced by paclitaxel, suggesting that ATF3(Δ C) may play a dominant-negative role for the induction of TAp73, but whether ATF3(Δ C) induced the mislocalization of TAp73 out of the nucleus was not exact at present although most of the TAp73 expressed moved to the nuclear membrane (Fig. 5D). Collectively, these results suggest that the COOH-terminal of ATF3 may be required for the translocation of ATF3 into the nucleus and ATF3 induced by paclitaxel might be an upstream regulator of TAp73. To confirm this, we examined whether TAp73 β overexpression reversibly affects ATF3 expression and translocation into the nucleus induced by paclitaxel (Fig. 6). Although endogenous TAp73 β expression was completely abolished by TAp73 β siRNA, paclitaxel-induced ATF3 expression was unchanged by overexpressing TAp73 β or inactive TAp73 β (Fig. 6B), supporting our findings that ATF3 is an upstream regulator of TAp73 β . Our data also showed that paclitaxel-induced apoptosis was strongly inhibited from TAp73 β depletion by TAp73 β siRNA (Fig. 6C), correlating with reduced ATF3 translocation into the nucleus (Fig. 6D). This suggests that TAp73 β might play an important role in apoptosis induced by paclitaxel-activated ATF3, supporting results that show a reduction of Bax and p21 expression and apoptosis from overexpressing ATF3(Δ C) and its restoration by GFP-TAp73 β overexpression, which was potentiated by cotreatment with paclitaxel (Fig. 7). Functional TAp73 β might be required for ATF3-mediated apoptosis and might be an important downstream effector for ATF3-mediated apoptosis. Hypothetically, ATF3 and TAp73 activation may be regulated reciprocally or in a positive feedback loop to induce the apoptosis of tumor cells. On the other hand, although ATF3 does not enter the nuclei in TAp73 β -depleted cells (Fig. 6D), the mechanism involved is still not clear. Recently, it was reported that TAp73 mediated the mitochondrial translocation of Bax proteins by transcriptionally inducing p53 up-regulated modulators of apoptosis involved in mitochondrial translocation (39). Thus, we cannot exclude the possibility that TAp73 β may also possibly induce a certain gene involved in the nuclear translocation of ATF3. Future experiments will be necessary to specify the underlying mechanisms involved in this phenomenon.

It is well established that the stability of tumor suppressor p53 is mainly controlled by mdm2, which binds to p53 and catalyzes ubiquitination degradation (13, 14, 22). In contrast, although TAp73 also binds to mdm2, their interaction does not lead to the proteosomal degradation of TAp73 (40). Nevertheless, the binding of TAp73 to mdm2 results in a dramatic inhibition of TAp73 transactivating activity (41). Recently, it was reported that ATF3 interacted and prevented p53 ubiquitination and degradation, consequently augmenting p53 function (25). Our data suggesting that endogenous ATF3 and TAp73 induced by paclitaxel interacts with each other *in vivo* includes a dose-dependent association between TAp73 β and GST-ATF3, but not with GST-ATF3(Δ C) or control GST beads. Moreover, these results indicate that stabilization of TAp73 β requires direct interaction with the COOH-terminal region of ATF3, and that the binding region of TAp73 β that was required for ATF3 interactions was a p73 β DNA-binding domain

(amino acids 54-310; Fig. 8). However, Δ Np73 β has opposing effects on apoptosis mediated by TAp73 because TAp73 β cotransfection, but not Δ Np73 cotransfection, highly induced apoptosis, which was potentiated by paclitaxel (Fig. 9D), although ATF3 interacts with the DNA-binding domain of TAp73 β (Fig. 9C), suggesting that the active TAp73 isoform was essential to induce apoptosis through paclitaxel-induced ATF3.

Therefore, we were interested in studying whether paclitaxel-induced ATF3 could also mediate TAp73 β 's stability by preventing ubiquitination degradation similar to p53. Our investigation showed that TAp73 β induction was enhanced slightly in MG132-pretreated cells and that overexpression of ATF3 alone increased TAp73 β expression (Fig. 9C), which was further potentiated by MG132 pretreatment. These effects were not observed in ATF3(Δ C)-overexpressing cells. Furthermore, our results show that ATF3 enhances TAp73 β 's stability by interfering with the ubiquitination of the latter (Fig. 9E and F). This event is achieved by direct interaction of the ATF3 with TAp73 β proteins, and deletion of the COOH-terminal domain in ATF3, which interacts with p53, failed to stabilize TAp73 β . Previously, we showed that the direct binding of p19Ras to TAp73 strongly enhanced tumor cell apoptosis by completely abolishing mdm2-mediated inhibition of TAp73 activity (34). Although the precise molecular mechanism behind the ATF3-dependent stabilization of TAp73 remains unknown, it is likely that ATF3 might also interact functionally with c-Abl, p300/CBP, or IKK- α , which are well known to interact with TAp73 (42-44). Furthermore, it is possible that there is another ubiquitin ligase, which is different from mdm2, that does not lead to the proteosomal degradation of TAp73 and instead contributes to the efficiency of TAp73 degradation. Among them, other E3 ligases specific for TAp73, such as ITCH, cannot bind TAp73 in the presence of ATF3. Further studies are needed to investigate the exact molecular mechanisms involved.

TAp73 stabilization has generally been shown to reflect an increase in its transcriptional levels (44). However, our results showed that paclitaxel did not lead to an increase in TAp73 β mRNA levels (Fig. 10A). We observed that ATF3 enhanced the stability of TAp73 β proteins induced by paclitaxel because TAp73 β decreased significantly by cycloheximide was attenuated by ATF3 overexpression (Fig. 10B). Following the stabilization of TAp73 β , ATF3 also enhanced the transactivation of p21 and Bax promoters downstream of TAp73 β as well as significantly inhibiting the TAp73-p21 binding complex in cells transfected with ATF3(Δ C) or ATF3 siRNA (Fig. 10C-F). These results suggest that the effects of ATF3 on paclitaxel-induced reporter activities could be due to the ability of ATF3 to increase the steady-state levels of TAp73 β via *de novo* protein synthesis. Chromatin immunoprecipitation analysis data shows that TAp73 β and ATF3 were efficiently recruited to the p21 and Bax promoters in control cells, which increased strongly in paclitaxel-treated cells. Furthermore, a significant increase in chromatin binding was higher in the presence of ATF3 than in cells transfected with GFP alone, supporting our previous findings showing that ATF3 enhanced the transcriptional activity of TAp73 β . Interestingly, ATF3 also binds to the same binding sites with TAp73 on p21 or Bax

promoters, but this recruitment of ATF3 to TAp73 binding sites was specific because we did not observe any amplification in STAT5 immunoprecipitated chromatin. These data suggest that ATF3 might directly bind to TAp73 binding sites or play as a cofactor mediating p73 functional activity because we have used the primers for TAp73-responsive element within the p21 or Bax promoter. However, we cannot exclude the possibility that ATF3 might interact indirectly, via association with TAp73, with the same regions containing TAp73 sites in p21 and Bax promoters because TAp73 and ATF3 interact with each other, whereas TAp73 interacts with the transcriptional coactivator p300 and CBP to enhance its function. Future experiments will be required to clarify the underlying mechanistic details of ATF3 functional interaction.

Another possibility is that ATF3 regulates the modification of TAp73 such as methylation because several studies using tissues from patients with cervical cancer show that TAp73 is often found hypermethylated, which correlated with reduced expression of TAp73 (45). According to our results, depletion of ATF3 impaired tumor suppressor TAp73 activation in response to paclitaxel. These findings could implicate ATF3 deficiency with the development of cancers, as the absence of ATF3 has been associated with activating a Ras signaling cascade and initiating carcinogenesis (21). This possibility was supported by our preliminary findings that TAp73 and ATF3 were expressed minimally in cervical cancer tissues compared with normal patient samples, but was significantly increased in paclitaxel-treated cervical cancer tissues, thereby reducing tumorigenesis (data not shown). Although there are an extensive number of independent regulations of TAp73 and ATF3, and ATF3 has been shown to be involved in TAp73 up-regulation in this study, the exact molecular mechanisms involved in ATF3 regulation of TAp73 activation and apoptosis are still unclear. The functional consequences of the interaction between ATF3 by paclitaxel and TAp73 up-regulation are likely to be complex and will require further study.

Finally, we provide novel insights into the mechanisms involved in paclitaxel-induced apoptosis through TAp73 up-regulation. We are the first to report that ATF3 is a novel activator of TAp73 function in p53-inactivated cells. We have shown that ATF3 plays an important role in regulating the apoptosis of cervical cancer cells via up-regulating TAp73 expression, which compensates for the cytotoxicity of p53 depleted by HPV E6.

Materials and Methods

Cell Line and Reagents

Cervical cancer HeLa cells containing p53 proteins inactivated by HPV E6 or HPV E7 oncogenes, human osteosarcoma SAOS2 cells with p53-null alleles, and human breast cancer MCF-7 cells with wild-type p53 alleles were obtained from American Type Culture Collection and cultured in DMEM containing 10% fetal bovine serum, 2 mmol/L of glutamine, and 100 IU/mL of penicillin, and 100 μ g/mL of streptomycin (Life Technologies). Anti-TAp73 α , anti-TAp73 β , anti-p53, anti-ATF3, anti-Bax, anti-Bcl-2, anti-Bcl-xL, anti-p21, anti-caspase-3, anti-poly(ADP-ribose) polymerase,

anti-cytochrome *c*, anti-GFP, and anti-flag were obtained from Cell Signaling Technology and Santa Cruz Biotechnology, Inc. *N*-acetyl-cysteine, phenylmethylsulfonyl fluoride, aprotinin, leupeptin, penicillin, streptomycin, propidium iodide, and other common chemicals were from Sigma. Paclitaxel (2 mg/kg/mL) and taxol (6 mg/mL paclitaxel in cremophor EL and dehydrated ethanol; Bristol-Myers-Squibb) were diluted with saline. To maximize the effects of ATF3 overexpression, the cells were incubated with a low concentration of paclitaxel (50 nmol/L).

Plasmids

Human wild-type ATF3 and mutated ATF3(Δ C; 1-100) with a COOH-terminal deletion cDNA expression vectors were generous gifts from Dr. T. Hai (Ohio State University, Columbus, OH). Human ATF3 and ATF3(Δ C) cDNA were amplified separately by PCR and cloned into pEGFP-C2 and pGEX-4T-1 vectors (Clontech). The pcDNA3-HA full-length TAp73 β construct was generously provided by Dr. Daniel Cauput (Sanofi Recherche, France). From pcDNA3-HA-TAp73 β , GFP-73 β was constructed by subcloning into the *Bam*HI/*Xba*I restriction sites of pEGFP-C1, pGL3-p21WAF1-luc, and pGL3-Bax-luc.

Transient Transfection

HeLa and MCF-7 cells were grown in six-well culture plates at ~60% to 70% confluence. Transfections were done/did using a Lipofectin reagent (Life Technologies) following the protocol recommended by the manufacturer. Briefly, after a 16-h incubation period, the medium was replaced with normal growth medium and cells were grown for an additional 24 h.

Immunoblots and Coimmunoprecipitation

Cells were lysed in radioimmunoprecipitation assay buffer [50 mmol/L Tris (pH 7.5), 1% Nonidet P40, 150 mmol/L sodium deoxycholate, 150 mmol/L NaCl, 1 mmol/L EDTA, 1 mmol/L sodium orthovanadate, 1 mmol/L sodium fluoride, 1 mmol/L phenylmethylsulfonyl fluoride, 1 μ g/mL aprotinin, 1 μ g/mL leupeptin, and 1 μ g/mL pepstatin] at 4°C, then vortexed and centrifuged at 16,000 rpm for 10 min at 4°C. The supernatant was mixed in Laemmli loading buffer, boiled for 4 min, and then subjected to SDS-PAGE. For immunocomplexes, whole-cell lysates (500 μ g) were immunoprecipitated with 2 μ g of antibody and immunoblotted.

Reverse Transcription-PCR Analysis

Total RNA was isolated from the cell lines using TRIzol reagent (Life Technologies) and reverse transcription-PCR analysis was done using a forward 5'-TCTGGAACCAGACAGCACCT-3' primer and a reverse 5'-GTGCTGGACTGCTGGAAAGT-3' primer. Actin was used for internal normalization.

GST Pull-down Assay

For *in vitro* binding assays, 500 μ g of lysates were incubated with 3.0 μ g of GST or fusion GST-GCK proteins coupled to glutathione Sepharose beads in 300 μ L of lysis buffer overnight at 4°C with continuous rocking as described previously (46).

Immunocytochemistry

The cells were grown on poly-D-lysine-coated coverslips in six-well plates. After treatment, cells were washed with PBS, and then fixed with 3.7% formaldehyde in PBS for 10 min at room temperature. The coverslips were soaked in a blocking solution (PBS containing 5% bovine serum albumin and 0.2% Triton X-100) for 30 min and incubated with anti-ATF and anti-p73 (1:300) overnight at 4°C and then with Alexa-488 anti-rabbit IgG antibody (1:400) for 30 min in the blocking solution before mounting. Fluorescence was analyzed by confocal microscopy (28).

Electrophoretic Mobility Shift Assay

DNA mobility shift assays were done in 20 μ L volumes with 20 mmol/L of Tris-HCl (pH 7.9), 1.5% glycerol, 50 μ g/mL bovine serum albumin, 1 mmol/L of DTT, 0.5 mmol/L of phenylmethylsulfonyl fluoride, 2 μ g of poly(deoxyinosinic-deoxycytidylic acid), 1 ng ³²P-labeled probe (5'-AGCTAGTAGAGCGAACATGTCCcAACATGTTgGCGTGCTGCAGC-3'), and 10 μ g of nuclear extract. Reactions were incubated at 25°C for 20 min and subsequently analyzed by electrophoresis through nondenaturing stock polyacrylamide gels (6% or 10%) in 0.5 \times Tris-borate EDTA buffer containing 44.5 mmol/L Tris-HCl (pH 8.2), 44.5 mmol/L boric acid, and 1 mmol/L EDTA. After the gel was prerun at 100 V for 2 h, electrophoresis was done at 270 V for 2 h at 4°C. The gels were exposed to X-ray films using two intensifying screens -70°C.

Luciferase Reporter Gene Assay

We did transient transfections by using the Lipofectin reagent (Life Technologies) as described previously (28). Briefly, the cells were washed twice with Opti-MEN 1 reduced-serum medium (Life Technologies) and 0.5 μ g of each plasmid DNA [pGL3-p21WAF1-luc, pGL3-Bax-luc, ATF3 cDNA, ATF3(Δ C), TAp73 β , and ATF3 siRNA or TAp73 siRNA] per 35 mm plate was cotransfected with 0.5 μ g of β -galactosidase vector (Promega) to allow for adjustments of transfection efficiencies. After transfection, the cells were incubated continuously in serum-reduced medium for 8 h, then changed to DMEM containing 2% serum. Cells were harvested after an additional 24-h period, lysed by freeze-thawing, and assayed for luciferase or β -galactosidase activities. We determined protein concentrations by using the Bio-Rad protein assay solution as described by the manufacturer, and bovine serum albumin as standard. We replicated all transfections at least thrice and found similar results.

RNA Interference and Transfection

ATF3 (sc-29757), p53 (sc-29435), and TAp73 siRNA (sc-36167, SC-37475, each 0.5 μ g) were purchased from Santa Cruz Biotechnology, and HeLa cells were plated at 50% to 70% confluence and transfected with siRNA complexes or only with transfection reagents using LipofectAMINE 2000 (Invitrogen).

Chromatin Immunoprecipitation

The chromatin immunoprecipitation assays were done following a protocol provided by Upstate Biotechnology, Inc.

In brief, H1299 cells were transiently transfected with the expression plasmids for GFP or GFP-ATF3 (0.5 μ g). Forty-eight hours after transfection, cells were cross-linked with 1% formaldehyde in medium for 15 min at 37°C. Cells were then washed with ice-cold PBS and resuspended in 200 μ L of SDS-sample buffer containing protease inhibitor mixture. The suspension was sonicated 10 times for 30 s with a 1-min cooling period on ice between times and precleared with 20 μ L of protein A-agarose beads blocked with sonicated salmon sperm DNA for 30 min at 4°C. The beads were removed and the chromatin solution was immunoprecipitated overnight with anti-ATF3, p73, and GFP monoclonal antibodies at 4°C, followed by incubation with protein A-agarose beads for an additional 1 h at 4°C. The immunocomplexes were eluted with 100 μ L of elution buffer (1% SDS and 0.1 mol/L NaHCO₃) and formaldehyde cross-links were reversed by heating at 65°C for 6 h. Proteinase K was added to the reaction mixtures and incubated at 45°C for 1 h. DNAs of the immunoprecipitates and control input DNAs were purified using a QIAquick PCR purification kit (Qiagen Inc.) and then analyzed by regular PCR using the human p21*WAF1* and *Bax* promoter-specific primers. The primer sequences were 5'-CACCTTTCACCATCCCTA-3' and 5'-GCAGCC-CAAGGACAAAATAG-3' for p21*WAF1* and 5'-AAAGCT-CAGAGGCCCAAAAT-3' and 5'-AGGCTGAGACGGG-GTTATCT-3' for *Bax*.

In vitro and In vivo Ubiquitination Assays

GST-TAp73 and GST-ATF3 proteins were expressed in *Escherichia coli* BL21, and purified with glutathione-agarose (Sigma). *In vitro* ubiquitination assays was done as described previously (25) with some modifications. Recombinant purified GST-TAp73 was preincubated with 250 ng of recombinant full-length or the deleted mutant ATF3 protein at 37°C for 1 h in a 30 μ L reaction buffer 1 containing 50 mmol/L of Tris-HCl (pH 7.5), 5 mmol/L of MgCl₂, 5 mmol/L of DTT, 4 mmol/L of ATP, 100 μ mol/L of E1, 10 μ mol/L of E2, 5 μ g His-ubiquitin (E1, E2, and His-ubiquitin were obtained from Boston Biochem), and His-ubiquitinated proteins were isolated by incubating at 4°C for 1 h with 20 μ L of nickel-nitrilotriacetate agarose (Qiagen) in a final volume of 200 μ L in reaction buffer 2 containing 50 mmol/L of sodium phosphate (pH 7.9), 300 mmol/L of NaCl, 0.05% Tween 20, and 10 mmol/L of imidazole. After low-speed centrifugation (735 \times g), the nickel-agarose beads containing His-ubiquitinated proteins were washed twice with 1 mL of reaction buffer 2. The nickel-bound proteins were eluted and then subjected to Western blotting for ubiquitinated p73 using anti-polyubiquitin antibody. *In vivo* ubiquitination assay was done as described previously (47) with some modifications. HeLa cells were cotransfected with the constant amount of HA-TAp73 (0.5 μ g) and His-tagged ubiquitin (0.5 μ g), together with the full-length ATF3 or the deleted mutant ATF3 (0.5 μ g). Forty hours after transfection, cells were treated with 20 μ mol/L of MG-132 for 6 h before being harvested. His-tagged ubiquitin-containing protein complexes were pulled down with nickel-agarose beads (Qiagen), and subsequently resolved by 10% SDS-PAGE, followed by immunoblotting with anti-HA antibody.

Statistical Analysis

For comparing values obtained in three or more groups, one-factor ANOVA was used, followed by Tukey's post hoc test, and $P < 0.05$ was taken to imply statistical significance.

Acknowledgments

We thank Dr. Van-Anh Nguyen for peer reviewing this article.

References

1. Arbuck SG, Dorr A, Friedman MA. Paclitaxel (Taxol) in breast cancer. *Hematol Oncol Clin North Am* 1994;8:121-40.
2. Foa R, Norton L, Seidman AD. Taxol (paclitaxel): a novel anti-microtubule agent with remarkable anti-neoplastic activity. *Int J Clin Lab Res* 1994;24:6-14.
3. Rowinsky EK. Paclitaxel pharmacology and other tumor types. *Semin Oncol* 1997;24:S19:1-12.
4. Xiao H, Verdier-Pinard P, Fernandez-Fuentes N, et al. Insights into the mechanism of microtubule stabilization by Taxol. *Proc Natl Acad Sci U S A* 2006;103:10166-73.
5. Nguyen DM, Yeow WS, Ziauddin MF, et al. The essential role of the mitochondria-dependent death-signaling cascade in chemotherapy-induced potentiation of Apo2L/TRAIL cytotoxicity in cultured thoracic cancer cells: amplified caspase 8 is indispensable for combination-mediated massive cell death. *Cancer J* 2006;12:257-73.
6. Woods CM, Zhu J, McQueney PA, Bollag D, Lazarides E. Taxol-induced mitotic block triggers rapid onset of a p53-independent apoptotic pathway. *Mol Med* 1995;1:506-26.
7. Bacus SS, Gudkov AV, Lowe M, et al. Taxol-induced apoptosis depends on MAP kinase pathways (ERK and p38) and is independent of p53. *Oncogene* 2001;20:147-55.
8. Kim YH, Shin SW, Kim BS, et al. Paclitaxel, 5-fluorouracil, and cisplatin combination chemotherapy for the treatment of advanced gastric carcinoma. *Cancer* 1999;85:295-301.
9. Irwin MS, Kaelin WG. p53 family update: p73 and p63 develop their own identities. *Cell Growth Differ* 2001;12:337-49.
10. Takagi S, Ueda Y, Hijikata M, Shimotohno K. Overproduced p73 α activates a minimal promoter through a mechanism independent of its transcriptional activity. *FEBS Lett* 2001;509:47-52.
11. Chen X, Zheng Y, Zhu J, Jiang J, Wang J. p73 is transcriptionally regulated by DNA damage, p53, and p73. *Oncogene* 2001;20:769-74.
12. Lin KW, Nam SY, Toh WH, Dulloo I, Sabapathy K. Multiple stress signals induce p73 β accumulation. *Neoplasia* 2004;6:546-57.
13. Zeng X, Chen L, Jost CA, et al. Mdm2 suppresses p73 function without promoting p73 degradation. *Mol Cell Biol* 1999;19:3257-66.
14. Honda R, Tanaka H, Yasuda H. Oncoprotein MDM2 is a ubiquitin ligase E3 for tumor suppressor p53. *FEBS Lett* 1997;420:25-7.
15. Dyson N, Howley PM, Munger K, Harlow E. The human papilloma virus-16 E7 oncoprotein is able to bind to the retinoblastoma gene product. *Science* 1989; 243:934-7.
16. Werness BA, Levine AJ, Howley PM. Association of human papillomavirus types 16 and 18 E6 proteins with p53. *Science* 1990;248:76-9.
17. Jost CA, Marin MC, Kaelin WG, Jr. p73 is a human p53-related protein that can induce apoptosis. *Nature* 1997;389:191-4.
18. Yamaguchi K, Lee SH, Kim JS, Wimalasena J, Kitajima S, Back SJ. Activating transcription factor 3 and early growth response 1 are the novel targets of LY294002 in a phosphatidylinositol 3-kinase-independent pathway. *Cancer Res* 2006;66:2376-84.
19. Latchman DS. Transcription factors as potential targets for therapeutic drugs. *Curr Pharm Biotechnol* 2000;1:57-61.
20. Hai T, Hartman MG. The molecular biology and nomenclature of the activating transcription factor/cAMP responsive element binding family of transcription factors: activating transcription factor proteins and homeostasis. *Gene* 2001;273:1-11.
21. Lu D, Wolfgang CD, Hai T. Activating transcription factor 3, a stress-inducible gene, suppresses Ras-stimulated tumorigenesis. *J Biol Chem* 2006;281: 10473-81.
22. Tamura K, Hua B, Adachi S, et al. Stress response gene ATF3 is a target of c-myc in serum-induced cell proliferation. *EMBO J* 2005;24:2590-601.
23. Fan F, Jin S, Amundson SA, et al. ATF3 induction following DNA damage is

- regulated by distinct signaling pathways and over-expression of ATF3 protein suppresses cells growth. *Oncogene* 2002;21:7488-96.
24. Mashima T, Udagawa S, Tsuruo T. Involvement of transcriptional repressor ATF3 in acceleration of caspase protease activation during DNA damaging agent-induced apoptosis. *J Cell Physiol* 2001;188:352-8.
25. Yan C, Lu D, Hai T, Boyd DD. Activating transcription factor 3, a stress sensor, activates p53 by blocking its ubiquitination. *EMBO J* 2005;24:2425-35.
26. Nobori K, Ito H, Tamamori-Adachi M, et al. ATF3 inhibits doxorubicin-induced apoptosis in cardiac myocytes: a novel cardioprotective role of ATF3. *J Mol Cell Cardiol* 2002;34:1387-97.
27. Hai T, Wolfgang CD, Marsee DK, Allen AE, Sivaprasad U. ATF3 and stress responses. *Gene Expr* 1999;7:321-35.
28. Kim WH, Lee JW, Gao B, Jung MH. Synergistic activation of JNK/SAPK induced by TNF- α and IFN- γ : apoptosis of pancreatic-cells via the p53 and ROS pathway. *Cell Signal* 2005;17:1516-32.
29. Goldschneider D, Blanc E, Raguenez G, et al. Differential response of p53 target genes to p73 overexpression in SH-SY5Y neuroblastoma cell line. *J Cell Sci* 2004;117:293-301.
30. Benjamin PC, Chen S, Guosheng L, James WO, Hai T. ATF3 and ATF3AZip. *J Biol Chem* 1994;269:15819-26.
31. Wu G, Osada M, Guo Z, et al. Δ Np63 α upregulates the HSP70 gene in human cancer. *Cancer Res* 2005;65:758-66.
32. Balint E, Bates S, Vousden KH. Mdm2 binds p73 α without targeting degradation. *Oncogene* 1999;18:3923-9.
33. Lohrum MA, Vousden KH. Regulation and function of the p53-related proteins: same family, different rules. *Trends Cell Biol* 2000;10:197-202.
34. Halder S, Jena N, Croce CM. Antiapoptosis potential of bcl-2 oncogene by dephosphorylation. *Biochem Cell Biol* 1994;72:455-62.
35. Kumar MV, Shirley R, Ma Y, Lewis RW. Role of genomics-based strategies in overcoming chemotherapeutic resistance. *Curr Pharm Biotechnol* 2004;5:471-80.
36. Faried LS, Faried A, Kanuma T, et al. Inhibition of the mammalian target of rapamycin (mTOR) by rapamycin increases chemosensitivity of CaSki cells to paclitaxel. *Eur J Cancer* 2006;42:934-47.
37. Kaghad M, Bonnet H, Yang A, et al. Monoallelically expressed gene related to p53 at 1p36, region frequently deleted in neuroblastoma and other human cancers. *Cell* 1997;9:809-19.
38. Park JS, Kim EJ, Lee JY, Sin HS, Namkoong SE, Um SJ. Functional inactivation of p73, a homolog of p53 tumor suppressor protein, by human papillomavirus E6 proteins. *Int J Cancer* 2001;91:822-7.
39. Melino G, Bernassola F, Ranalli M, et al. p73 induces apoptosis via PUMA transactivation and Bax mitochondrial translocation. *J Biol Chem* 2004;279:8076-83.
40. Jeong MH, Bae JH, Kim WH, Yoo SM, Kim JW, Song PI, Choi KH. P19Ras interacts with and activates p73 by involving the MDM2 protein. *J Biol Chem* 2006;281:8707-15.
41. Calabro V, Mansueto G, Parisi T, Vivo M, Calogero RA, La Matia G. The human MDM2 oncoprotein increases the transcriptional activity and the protein level of the p53 homolog p63. *J Biol Chem* 2002;277:2674-81.
42. Zeng X, Li X, Miller A, et al. The N-terminal domain of p73 interacts with the CH1 domain of p300/CREB binding protein and mediates transcriptional activation and apoptosis. *Mol Cell Biol* 2000;20:1299-310.
43. Costanzo A, Merlo P, Pediconi N, et al. DNA damage-dependent acetylation of p73 dictates the selective activation of apoptotic target genes. *Mol Cell* 2002;9:175-86.
44. Furuya K, Ozaki T, Hanamoto T, et al. Stabilization of p73 by nuclear κ B kinase- α mediates cisplatin-induced apoptosis. *J Biol Chem* 2007;282:18365-78.
45. Liu SS, Leung RC, Chan KY, et al. p73 expression is associated with the cellular radiosensitivity in cervical cancer after radiotherapy. *Clin Cancer Res* 2004;10:3309-16.
46. Amini S, Saunders M, Kelley K, Khalili K, Sawaya BE. Interplay between HIV-1 Vpr and Sp1 modulates p21(WAF1) gene expression in human astrocytes. *J Biol Chem* 2004;279:46046-56.
47. Lee K, Wang D, Lippard SJ, Sharp PA. Transcription-coupled and DNA damage-dependent ubiquitination of RNA polymerase II *in vitro*. *Proc Natl Acad Sci U S A* 2002;99:4239-44.